Journal of the Geological Society, London, Vol. **164**, 2007, pp. 895–921. Printed in Great Britain.

Bicentennial Review

Neoproterozoic glaciation in the Earth System

IAN J. FAIRCHILD[1] & MARTIN J. KENNEDY[2]
[1]*School of Geography, Earth and Environmental Sciences, University of Birmingham, Edgbaston, Birmingham B15 2TT, UK (e-mail: i.j.fairchild@bham.ac.uk)*
[2]*Department of Earth Science, University of California Riverside, Riverside, CA 92521, USA*

Abstract: The Neoproterozoic contains severe glacial intervals (750–580 Ma) including two extending to low palaeomagnetic latitudes. Paucity of radiometric dates indicates the need for chronostratigraphic tools. Whereas the marine $^{87}Sr/^{86}Sr$ signatures show a steady rise, $\delta^{13}C$ fluctuates, the most reproducible variations being negative signatures in carbonate caps to glacial units, but more diagenetic work is needed. Four conceptual models for the icehouse conditions are contrasted: Zipper-Rift Earth (diachronous glaciation related to continental rift margins), High-tilt Earth (high-obliquity and preferential low-latitude glaciation), Snowball Earth (extreme glaciation related to runaway ice–albedo feedback) and Slushball Earth (coexistence of unfrozen oceans and sea-level glaciers in the tropics). Climate models readily simulate runaway glaciation, but the Earth may not be able to recover from it. The Slushball state requires more extensive modelling. Biogeochemical models highlight the lack of CO_2 buffering in the Neoproterozoic and the likely transition from a methane- to a CO_2-dominated climate system. Relevant processes include tropical weathering of volcanic provinces, and new land biotas stimulating both clay mineral formation and P delivery to the oceans, facilitating organic C burial. Hence a step change in the Earth System was probably both facilitated by organisms and responsible for moderating Phanerozoic climate.

The foundation of the Geological Society in 1807 followed closely on James Hutton's field demonstration in 1785 of the reality of deep (geological) time (Craig 1997). Hutton took pleasure in contemplating the physiology of the planet, which he regarded as a 'compound system of things, forming together one whole living world' (McIntyre & McKirdy 2001). Now planetary physiology is back on the agenda, following the thinking of the Society's 2006 Wollaston medallist James Lovelock (Lovelock 1988). Earth System Science represents the mainstream scientific effort equivalent to Lovelock's Gaia theory, but without a search for an underlying purpose (Lovelock 2006). Such concerns with global cycling and feedbacks, and in particular Paul Hoffman's vigorous advocacy of the Snowball Earth hypothesis (Hoffman *et al*. 1998; Hoffman & Schrag 2000, 2002), have generated excitement in the field of study of Precambrian glaciation (Walker 2003). More soberly, Earth System approaches have provided a medium by which to develop Hutton's gift of testing conjectures in historical science by making verifiable predictions.

For newcomers to the complex Neoproterozoic literature, we have tried to emphasize the more firmly accepted information and highlight those differences in interpretation that are still current. We illustrate that age-uncertainties are still significant in permitting different interpretations of the stratigraphic record, and hence stimulating vigorous debate, but also that carbonate rocks reveal vital information on global elemental cycling and climate. Three mutually exclusive viewpoints on the extent and significance of Neoproterozoic glaciation (Snowball Earth, High-tilt Earth and Zipper-Rift Earth) are contrasted with a more pragmatic synthesis of the most extreme glacial state, Slushball Earth (Fig. 1). We show how quantitative climatic and biogeochemical models constrain the state of the Earth System, and suggest the types of research that will reduce the uncertainties.

Geological evidence

Although the Neoproterozoic is defined to range from 1000 Ma to the start of the Cambrian (542 Ma, Amthor *et al*. 2003), there is no evidence of glaciation before *c*. 750 Ma or after *c*. 580 Ma. Glaciation occurred not only in the eponymous Cryogenian (defined to start at 800 Ma, Plumb 1991), but also in the succeeding Ediacaran Period, which is defined to begin above a glacial unit in Australia (Fig. 2f), correlated with sections in China (Fig. 2g and h) and Namibia dated at *c*. 635 Ma (Knoll *et al*. 2006).

Glacial deposits in Neoproterozoic sedimentary basins

The first record of glacial deposits now known to be Precambrian was of 'pebbles and boulders of granite in schistose rocks in Islay, Scotland' by James Thomson in 1871 (Spencer 1971). The exotic appearance of the rock (Fig. 2b) was later shown by Spencer (1971) to be matched by evidence that the clasts originated from a different source than that which supplied other levels in this Dalradian Neoproterozoic succession. Distinctive provenance is a characteristic of glaciated basins, and together with the use of other criteria developed from modern and Quaternary glacial environments, such as faceted and striated clasts indicative of subglacial transport, or dropstones and till pellets derived from floating ice, a picture of the distribution of past glacial activity emerges from detailed facies analysis (Hambrey & Harland 1981).

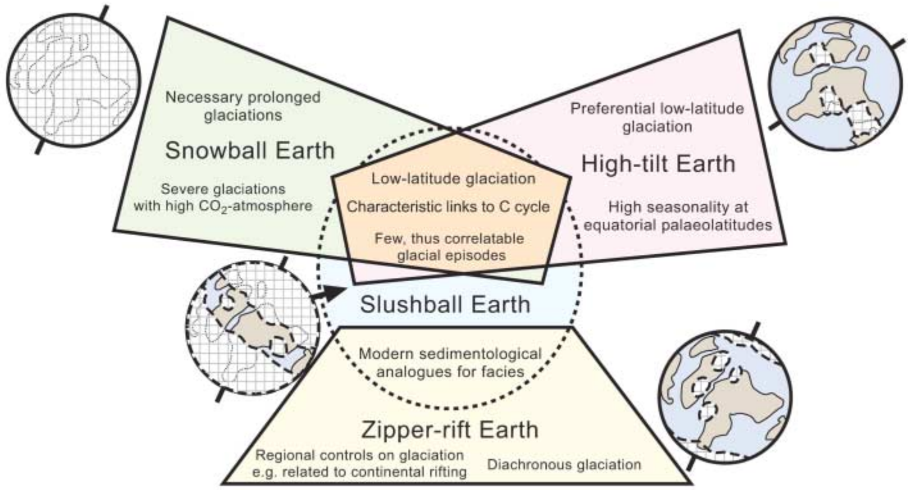

Fig. 1. Venn diagram illustrating the essential differences in interpretation used to supportive contrasting views of Neoproterozoic glaciation. For example, the Snowball and High-tilt models are distinct, although they accept some evidence in common, as illustrated. Distribution of ice in sketch maps is shown by cross-hatched ornament.

During the first half of the 20th century, the worldwide distribution of evidence of Proterozoic glaciation (Fig. 3) gradually became apparent in the context of a quite sophisticated awareness of possible controlling mechanisms (Coleman 1926). Many workers referred to glacigenic stratigraphic units as tillites (i.e. originally thought of as being laid down directly from ice), but this term has been less used lately because many glacigenic deposits grade into non-glacial sediment, or become redeposited, and many till-textured rocks (diamictites) are not connected with glaciation. Kulling (1934) drew on his work in Svalbard in comparison with discoveries of tillites and 'tillitiferous sediment-series' in China, Australia, North America, India, central Africa and Siberia to suggest 'that the eo-Cambrian glaciation probably was comparable in magnitude to that of the Permo-Carboniferous and Quaternary glaciations', although claims of the extent of glaciation were confused by uncertainty over timings of glaciation and a reluctance to accept continental drift (Coleman 1926; Mawson 1949).

As summarized in the global synthesis of Hambrey & Harland (1981), in any one region there may be one, two or exceptionally three discrete glacial formations or equivalent evidence of glaciation (Fig. 3), but they always represent only a small percentage of the thickness of Neoproterozoic sediments. Glacial units are typically overlain by a cap carbonate (Fig. 2a, f and g) with a negative $\delta^{13}C$ signature. Cap carbonates have been given prominence when considering the Earth System relationships of glaciation (Kennedy 1996; Hoffman *et al*. 1998), because of their widespread occurrence, specific characteristics, and the possibility that they provide a physical record of perturbations in the global carbon cycle.

Following the simplifying synthesis of Kennedy *et al*. (1998) and subsequent radiometric determinations, a current view (Hurtgen *et al*. 2005; Halverson 2006) is that there are three groupings of timings of major glaciation (Fig. 3): Sturtian (<740–647 Ma, type location South Australia), Marinoan (<660–635 Ma, type location South Australia) and Gaskiers (*c*. 580 Ma, type location Avalonian Newfoundland, Canada). The geographical distribution of alleged Marinoan deposits is widest, including low-palaeolatitude examples (Fig. 3b), and that of Gaskiers deposits is least (Fig. 3c). Older literature often refers to a Varangian (type location North Norway), rather than Marinoan glaciation, but this has been discarded because of uncertainties of the ages of glacial events in the North Atlantic region. Further change in terminology is likely given the small time-gap (<10 Ma) in recent results (Condon *et al*. 2005; Kendall *et al*. 2006) between Sturtian of South Australia (Kendall *et al*. 2006) and supposed Marinoan correlatives (Condon *et al*. 2005). Although the lithological similarity of cap carbonates and chemostratigraphic correlations continues to support correlation of glacial horizons between basins, radiometric ages have not yet been able to substantiate this critical relationship, and the growing number of discordant ages in the lower glacial interval allows the possibility of a diachronous origin during a protracted ice age.

There is a large literature examining the context and sedimen-

Fig. 2. Neoproterozoic glacial deposits and associated carbonate facies. (**a**) Polarisbreen, NE Spitsbergen. Neoproterozoic section including the glacigenic Wilsonbreen Formation (arrowed), underlain by a regressive peritidal dolomite (1, see also (**e**)), and capped by a transgressive cap dolomite (3). Level 2 (see also (**c**) and (**d**)) corresponds to a complex of glacilacustrine facies. (**b**) Diamictite with granite clasts in cleaved matrix, Port Askaig Tillite (Garvellachs, Scotland), bed 38 of Spencer (1971), the same level as at the type site at Port Askaig, Islay; variously interpreted as terrestrial glacial and glacimarine (Arnaud & Eyles 2006; Benn & Prave 2006). (**c**) and (**d**) Mid-Wilsonbreen glacilacustrine facies. (**c**) Photomicrograph of fibrous cement crusts in stromatolitic limestone (stained pink by Alizarin Red-S) being broken into intraclasts in shallow turbulent water (view 6 mm wide). (**d**) Sandy diamictite overlain by silt–limestone couplets (varves). (**e**) Cathodoluminescence image of early cemented peritidal oolitic dolostone (Slangen Member) truncated by quartz sand (black) filling periglacial fractures at the base of the Wilsonbreen Formation (view 2 mm wide). (**f**) The Global Stratotype Section and Point for the Ediacaran Period at the base of the cap carbonate (Nuccaleena Formation) at this outcrop in the Flinders Ranges of South Australia (see also Raub *et al*. 2007). Arrow indicates the sharp contact with the underlying Elatina Formation, the Marinoan-aged glacial deposit. (**g**) and (**h**) the *c*. 635 Ma cap carbonate overlying the Nantuo Formation in south China. The arrow in (**g**) points to the base of the cap carbonate, and the disrupted and heavily cemented bedding is enlarged in (**h**). This texture was described by Jiang *et al*. (2003) and records $\delta^{13}C < -40‰$ indicative of carbon derived from methane oxidation. (**i**) Cap carbonate showing heavy carbonate cementation and non-tectonic buckling (Keilberg Fm.) overlying the *c*. 635 Ma Ghaub Fm. of northern Namibia. Similar structures are present in cap carbonates in Australia, Norway and the southwestern USA. (**j**) Tepee-like structures of a different origin from (**i**) in the Nuccaleena Formation of South Australia show vertical offset of a linear anticlinal axis (Kennedy 1996) similar to structures attributed by Allen & Hoffman (2005) to giant wave ripples (penknife for scale). Laterally, these structures are similar to nonlinear, heavily cemented structures in (**h**) and (**i**).

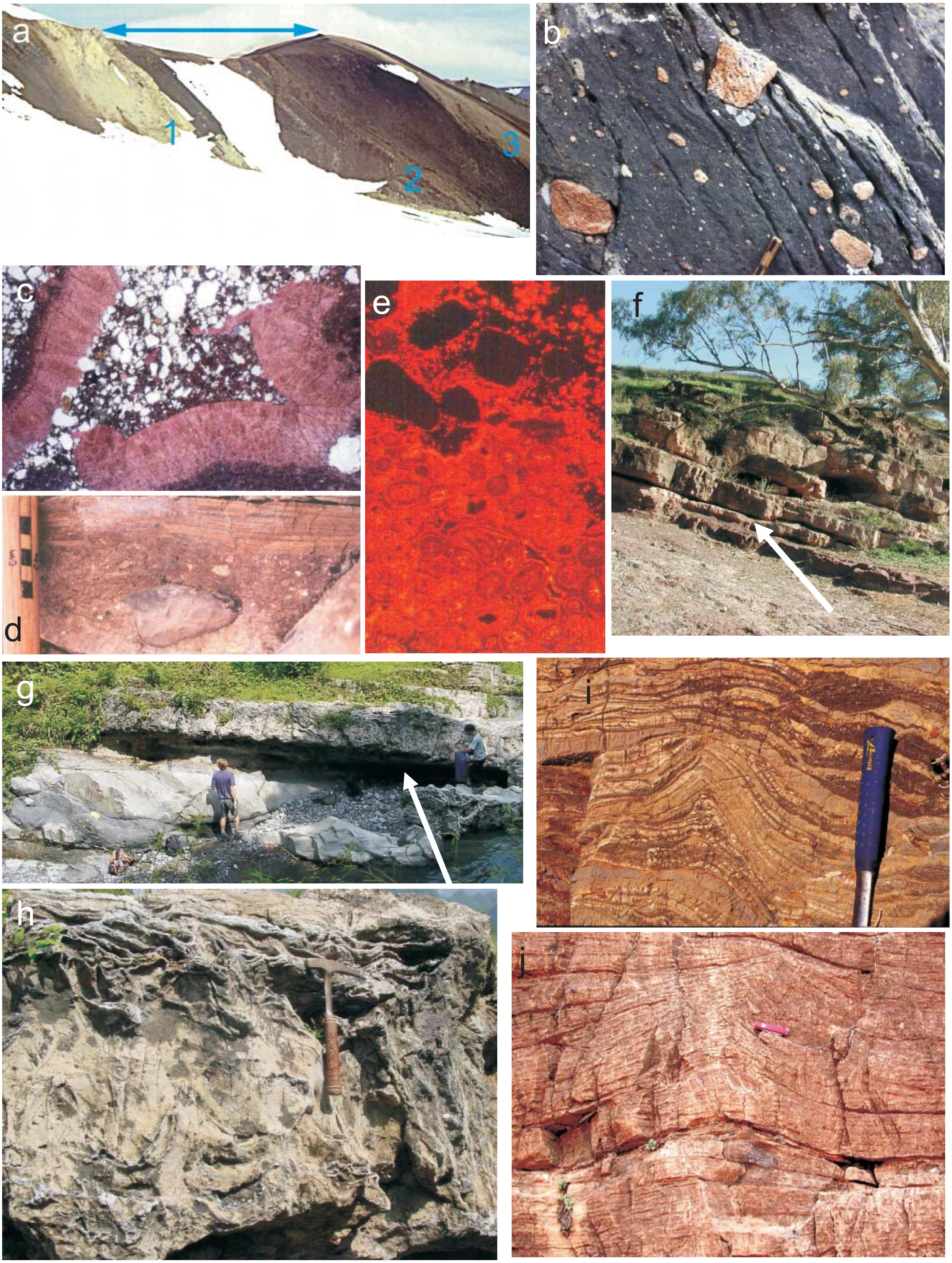
a
1
2
3
b
c
d
e
f
g
h
i
j

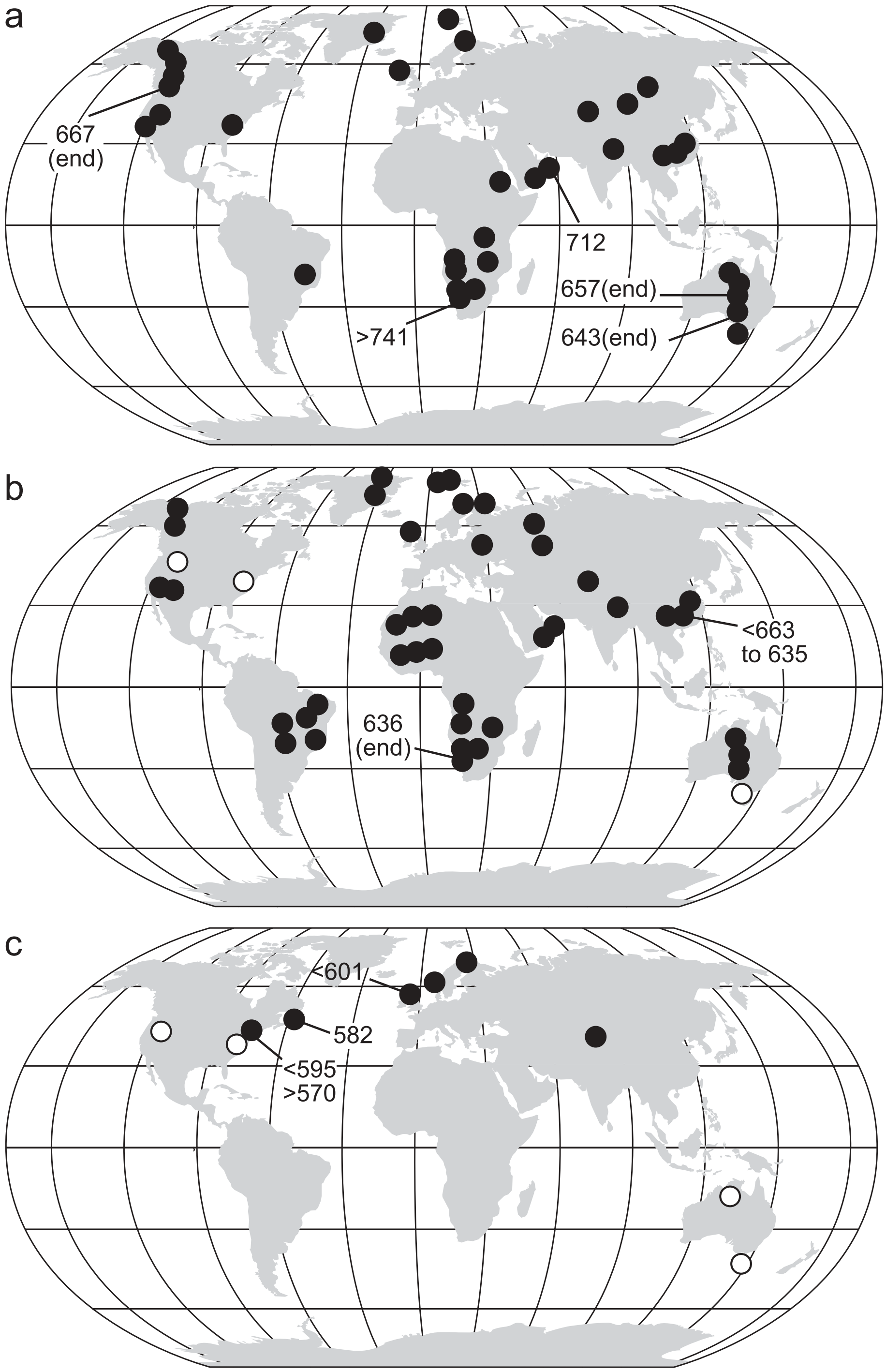

Fig. 3. Geographical distribution of Neoproterozoic alleged glacial deposits grouped by age (modified from Halverson 2006) with critical age constraints. In most cases, the assignment to a given interval is based on stratigraphic or loose geochronological constraints and/or the occurrence of a cap carbonate with distinctive characteristics. Some uncertain assignments are shown as open circles. (**a**) Period 740–660 Ma ('Sturtian'). More and less certain assignments are not distinguished. Age constraints from Namibia (Frimmel *et al*. 1996), Idaho (Fanning & Link 2004), Oman (Brasier *et al*. 2000) and Australia (Kendall *et al*. 2006). (**b**) Period <660 to 635 Ma ('Marinoan'). Age constraints from Yangtze Platform, China (Condon *et al*. 2005) and from central Namibia (Hoffmann *et al*. 2004). Despite the apparently widespread nature of Marinoan deposits, assignment of the Scottish Port Askaig Formation (Fig. 2b) and its Irish equivalents to the Sturtian by Condon & Prave (2000) and Brasier & Shields (2000) leaves no Marinoan representative in the UK, although a new discovery has been made in Ireland (McCay *et al*. 2006). (**c**) Ediacaran glacial deposit ('Gaskiers'), e.g. 580 Ma. Age constraints from Massachusetts (Thompson & Bowring 2000), Newfoundland (Bowring *et al*., unpublished, cited by Halverson 2006) and Scotland (Dempster *et al*. 2002). Strong stratigraphic arguments also favour a Gaskiers age for the Mortesnes deposits in northern Norway and Hankalchough in NW China (Halverson *et al*. 2005).

tological characteristics of the alleged glacigenic units, which are typically preserved by subsidence in synrift or post-rift basins. The necessity of active production of accommodation space must necessarily bias the completeness of the Neoproterozoic record to tectonically active areas. Where tectonically influenced depositional slopes do not dominate the geometry of sedimentary facies, sections of shallow marine to coastal non-glacial facies are interrupted by complex interdigitations of glacimarine and/or terrestrial glacial facies (e.g. NE Svalbard, Fairchild & Hambrey 1984; West African Craton, Deynoux 1985). Many sections show evidence of phases of relative ice advance and retreat (Spencer 1971; Lindsay 1989; Leather *et al*. 2002). Close analogies with modern glacial environments of various thermal regimes have been suggested: ranging from high sedimentation rates of the Neogene glacimarine Gulf of Alaska setting (Eyles & Eyles 1983), to ice-stream-fed ice shelves of parts of the modern Antarctic margin (Moncrieff & Hambrey 1990; Fig. 4c), to the hyper-arid Dry Valleys of Antarctica (Fairchild *et al*. 1989).

The similarities and differences between Neoproterozoic and Phanerozoic glacial deposits provide important clues to the dominant climate controls. Do Neoproterozoic glacial deposits contain sedimentary features indicative of different dominating

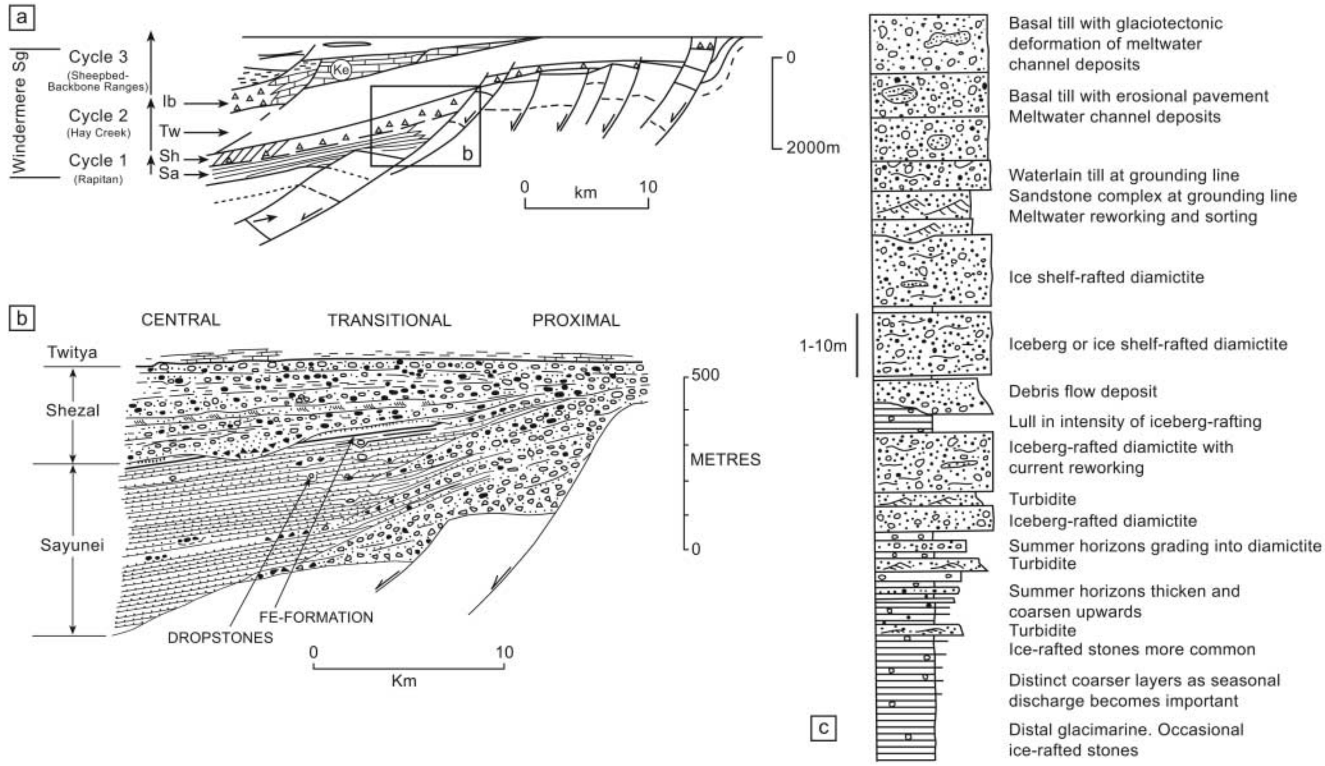

Fig. 4. Glacial facies relationships. (**a**) Reconstruction of part of rifted Laurentian margin of NW Canada (Windermere Supergroup, Mackenzie Mountains) illustrating the preferential occurrence of two glacial units downslope of synsedimentary faults. (**b**) Enlargement of part of (**a**) illustrating the redeposition of glacial sediment as sediment gravity flows. (**a**) and (**b**) are after Eisbacher (1985), Aitken (1991*a*), Eyles (1993) and Eyles & Januszczak (2004). (**c**) Sedimentation model illustrating coarsening-upwards succession from laminites to diamictites of different types resulting from the advance of a marine ice front, based on Neoproterozoic examples from East Greenland (after Moncrieff & Hambrey 1990).

mechanisms acting on the Earth System or are they largely similar to what is known from the Quaternary and Phanerozoic in general? For example, the strong positive feedback inherent in the albedo driver proposed in the Snowball Earth model should produce a rapid-in and rapid-out monotonic stratigraphic record lacking the high-frequency sea-level variation characteristic of the more delicately balanced feedbacks acting in the Quaternary. The seemingly abrupt and synchronous termination of the Marinoan glaciation (Condon *et al*. 2005) in China and Namibia would suggest this difference, whereas the repeated alternations of glacial and non-glacial facies reported in some Neoproterozoic formations would stress the similarity to the Quaternary (Condon *et al*. 2002; Leather *et al*. 2002; Arnaud & Eyles 2006). In their overview of Neoproterozoic glacial deposits, Etienne *et al*. (2007) found that the styles of preservation of glacial facies can all be matched with Phanerozoic examples and that there are no characteristics requiring extreme frigidity.

Where active rifting occurred, redeposition on slopes can mask the evidence of glacial activity. Across rifted margins, glacigenic strata are preferentially preserved in hanging-wall positions where it is can be expected that there has been major redeposition by mass flows (Eyles 1993; Eyles & Januszczak 2004). It is notable that hematitic Banded Iron Formation, not otherwise known since around 2 Ga, occurred in such settings (Fig. 4a and b), an association that Young (2002) linked to contemporary hydrothermal activity associated with basaltic volcanism during basin extension. Whether or not there is a glacial imprint on a given sedimentary succession dominated by mass flows can be debatable (Dott 1963; Schermerhorn 1974; Hambrey & Harland 1981; Eyles 1993). The latest sedimentological studies have the benefit of advances in understanding of ice-sheet dynamics on the one hand and subglacial sediment deformation on the other (Etienne *et al*. 2007), yet significant differences in interpretation can remain. An example is the disputed relative importance of subglacial (Spencer 1971; Benn & Prave 2006), glacimarine (Eyles & Eyles 1983) and marine slope (Arnaud & Eyles 2002, 2006) processes on the Scottish Port Askaig deposits. The upshot of this research is a consensus that widespread Neoproterozoic glaciation occurred, but that its influence is disputed in a number of individual cases. It continues to be important to document as many sedimentary features commonly associated with glaciation as possible (e.g. Thomas & Connell 1985), recognizing that no single feature is diagnostic.

Carbonate facies

Carbonates capture key geochemical and climatic information that constrain the state of the contemporary Earth System. Their deposition in the oceans throughout the sedimentary record is a response to the delivery of solutes derived primarily from terrestrial weathering. Whereas Proterozoic carbonate platforms were geometrically similar to those of the Phanerozoic (Grotzinger & James 2000) depositional controls on carbonates differed prior to the advent of skeletal precipitation. For example, the absence of pelagic calcifiers in the Precambrian means that there was no buffering of atmospheric CO_2 by variable dissolution of deep-sea carbonate ooze, as found today (Ridgwell *et al*. 2003). Both the absence of obligate calcifiers in the ocean and the occurrence of unusual carbonate sedimentary structures such as former-aragonite crystal fans point to high carbonate saturations of seawater (Grotzinger & Knoll 1995; Sumner 2001). However, saturation states vary spatially, and $CaCO_3$ precipitation would have been focused where processes such as net warming or evaporation, photosynthetic withdrawal of carbon dioxide, or heterogeneous nucleation by microbial cell matter occurred (Knoll & Swett 1990; Fairchild 1991; Riding 2000; Bosak & Newman 2003; Wright & Oren 2005) resulting in stromatolitic, micritic, intraclastic–peloidal and oolitic facies. Pure carbonate sediments accumulate where the supply of siliciclastic detritus is minimized, particularly on isolated platforms, or in relatively arid environments or where kinetic barriers to carbonate precipitation are breached, such as at the chemocline or in microenvironments promoted by microbial metabolism. Thick carbonate platform successions imply high rates of carbonate production to keep pace with thermal subsidence and so, in principle, are favoured in the tropical to sub-tropical belts, where rates of evaporation are highest. Although no definitive latitudinal or temperature limits on carbonate development can be given (carbonate sediments are common at all latitudes in the modern world), certain structures such as ooids (but not pisoids, James *et al*. 2005), and thick displacive cement crusts associated with tepees in peritidal sediments, are particularly suggestive of rapidly evaporating, warm conditions (Fairchild & Hambrey 1984; Knoll & Swett 1990). Carbonate platform deposits with such characteristics can be found immediately beneath glacigenic units (Fig. 2e): the crux of the palaeoclimatological paradox summarized in Fairchild (1993).

Mixed carbonate–siliciclastic facies, although unusual in the Phanerozoic, are remarkably common in Precambrian coastal, carbonate ramp and platform slope environments, and are of dolomitic, calcitic, or dual carbonate mineralogy. The origin of the carbonate in such facies is much more variable, including detrital, primary marine precipitates, and secondary phases in various diagenetic environments.

An important example of early diagenetic effects is provided by the matrix of diamictites. Carbonate in glacial facies is predominantly detrital, yet carbonate in the diamictite matrix can differ in composition from the larger clasts, having negative $\delta^{13}C$ values (Crossing & Gostin 1994; Kennedy *et al*. 2001*b*), and enrichment in Fe (visible on weathered rock surfaces) and Mn; in some cases there is a positive $\delta^{18}O$ signature (Fairchild *et al*. 1989). The closest modern analogue to such facies is provided by weakly lithified late Quaternary clast-rich deposits (analogous to the Heinrich layers of the North Atlantic) recovered from piston cores in the Arctic Ocean (Clark *et al*. 1980) where ice-rafted dolomite is the main detrital mineral, but key differences are found in the Neoproterozoic. Walker (1996) demonstrated, by deconvolving the geochemistry of Arctic ocean sediments composed principally of detrital dolomite mixed with Foraminifera, that there was an authigenic component, which, when separated, was found to form lozenge-shaped crystals of intermediate-Mg (6–7 mol% $MgCO_3$) calcite. In the modern case, the detrital dolomite was already hundreds of millions of years old and mineralogically stable and so was not prone to recrystallization. In contrast, these Neoproterozoic glaciers eroded freshly formed dolomitic carbonates, highly susceptible to recrystallization, for example by crystal ripening (Fairchild 1993).

Carbonate deposits occur in Quaternary continental deposits associated with glacial sediments, and can precipitate by freezing, aqueous or benthic photosynthesis, as well as skeletonization, and interglacial redeposition under organic soils (Fairchild *et al*. 1994). Neoproterozoic examples include the synglacially redeposited carbonates from North Africa described by Deynoux (1985). The best-developed occurrence (Fairchild *et al*. 1989) is an assemblage of carbonate facies from the Wilsonbreen Formation of Svalbard (Fig. 2a, c and d) including limestone and dolomite stromatolites, clastic–carbonate rhythmite couplets, dolocretes and evaporite pseudomorphs, intimately associated with sandstones and diamictites, which compare closely with the modern Antarctic Dry Valleys region. These carbonates include an evaporative stromatolite with the heaviest oxygen of any ancient carbonate rock (Fairchild *et al*. 1989), reanalyses of which in current work indicate compositions up to +15‰ (V-PDB). This can only be accounted for by hyper-arid conditions. The primary glacial meltwaters were not strongly depleted in ^{18}O as in the modern case, but originated from truncated atmospheric trajectories, with limited Rayleigh fractionation of atmospheric moisture (Fairchild *et al*. 1989), consistent with low-latitude glacial conditions. In contrast, in the Australian Olympic Formation and the Californian Kingston Peak Formation, there are occurrences of a wider variety of carbonate facies types within an overall glacial context (Kennedy *et al*. 2001*b*; Corsetti & Kaufman 2003), which contradict the generalization of Fairchild (1993) that typical carbonate platform facies types are only found bounding glacial units.

Cap carbonates and deglaciation

The close association between glaciation and carbonate deposition has been most widely studied in post-glacial capping carbonates that are all but ubiquitous in Neoproterozoic glacial successions (Williams 1979; Fairchild 1993; Kennedy *et al*. 1998; James *et al*. 2001; Hoffman & Schrag 2002; Shields 2005). These thin (<5 m) dolomite horizons sharply overlie glacigenic facies (Fig. 2a, f and g), and are persistent at basinal to inter-basinal scales. Where several discrete glacial intervals occur in a single succession, each is commonly overlain by a cap carbonate that may constitute the only carbonate within an otherwise siliciclastic succession. A conformable contact between glacigenic deposits and cap carbonates in most formations implies a genetic relation between glaciation and carbonate deposition, rather than simply carbonate deposits temporally separated but in physical contact with glacigenic sediments. The stratigraphic repetition, lateral continuity, and abrupt change to and from carbonate deposition has focused attention on cap carbonates as a physical record of a recovery from a global carbon cycle sufficiently perturbed to result in low-latitude glaciation (Kennedy 1996; Hoffman *et al*. 1998; Ridgwell *et al*. 2003) and one that lacks direct analogues in the Phanerozoic glacial record. This difference is further reinforced by the seemingly instantaneous termination of glacial facies (e.g. glacial features such as dropstones are largely absent from cap carbonates) with transgressive carbonate deposition that contrasts with the numerous waning glacial–interglacial cycles of the Phanerozoic deglacial record. Abrupt glacial termination is consistent with the lateral persistence of caps and suggests that they record glacio-eustasy (Preiss *et al*. 1978; Kennedy *et al*. 1998; Condon *et al*. 2005).

That cap carbonates are evidence for differences in Precambrian climate controls is further suggested by their petrology and geochemistry. The vast majority of cap carbonate exposures show 1–5 m of mechanically laminated, thinly bedded microcrystalline dolomite (in some cases composed of <50 μm graded peloids) hemipelagic deposits in shelfal environments. However, in almost all basins where cap carbonates are preserved, local exposures show an assemblage of peculiar sedimentary structures, including tepee-like antiforms (Fig. 2h–j) of several different morphologies and origins (Aitken 1991*b*; James *et al*. 2001; Allen & Hoffman 2005; Gammon *et al*. 2005; Jiang *et al*. 2006), aragonite fans (James *et al*. 2001; Hoffman & Schrag 2002), parallel vertical tube-like structures (Cloud *et al*. 1974; Hegenberger 1993; Corsetti & Grotzinger 2005), sheet cracks (Kennedy 1996; Jiang *et al*. 2006), and baritic and iron oxide crystal fans indicative of condensation at the top of the unit (Walter & Bauld 1983; Kennedy 1996). There is often a shift from microcrystalline, fabric-retentive dolomite to calcite. The origin of these structures is likely to be important for understanding the enigma of cap carbonates because, although locally developed, they occur in almost all global examples, and where two cap carbonate intervals occur within a succession, they each show a distinctive collection of sedimentary structures reproducible globally.

Cap carbonates record carbon isotope values that show depletion in $\delta^{13}C$ up-section. The $\delta^{13}C$ of the cap carbonate has played an important role both in forming models for the origin of cap carbonates and in correlating the unit between basins and arguing for its global synchronicity. The similarity of the $\delta^{13}C$ values between basins and the systematic trend, which typically begins around 0‰ and declines to as low as −6‰, is used as evidence that these values record a secular change in seawater that can be correlated globally, and is sufficiently accepted to serve as one of the defining features of the base of the Ediacaran Period (Knoll *et al*. 2006). Whereas negative isotopic values are reproducible, the magnitude and range of values can vary strongly from section to section as well as at millimetric scales (Jiang *et al*. 2006), suggesting that bulk values may represent an averaging of pore- and ocean-scale influences. The strong covariation between $\delta^{13}C$ and $\delta^{18}O$ in almost all cap carbonates, their dolomite mineralogy, evidence of recrystallization, the unknown origin of most carbonate grains, abundance of diagenetic cements, and the wide scatter in isotopic values where numerous sections have been analysed, or that are not completely dolomitized, further suggest that a combination of primary and diagenetic processes may be important in determining the bulk-rock value of cap carbonates (Jiang *et al*. 2006). These caveats also apply to the interesting discovery of stratigraphic variations in B and Ca isotopes (Kasemann *et al*. 2005). The secular (surface ocean) origin of the C isotopic excursion is a topic of active discussion with several possible mechanisms including Rayleigh fractionation of the atmosphere (Hoffman *et al*. 1998), temperature- or alkalinity-controlled fractionations (Higgins & Schrag 2003), upwelling of $\delta^{13}C$-depleted deep water (Grotzinger & Knoll 1995), or methane hydrate destabilization (Kennedy *et al*. 2001*a*; Jiang *et al*. 2003). That the isotopic excursion does not uniquely coincide with the cap carbonate, and may continue well up-section (after cap carbonate deposition ceased) opens the possibility that the two may be decoupled.

Critical to understanding cap carbonate implications and mechanisms is the duration of cap deposition; specifically, whether cap carbonates record reallocation of carbon already in the biosphere (non-steady state) or long-term derivation and deposition of carbon (steady state). Interpretations of timing range from condensed slow sedimentation (Kennedy 1996) to rapid whitings on the scale of hundreds to tens of thousands of years (Grotzinger & Knoll 1995; Hoffman *et al*. 1998; Kennedy *et al*. 2001*a*; Shields 2005). However, numerous palaeomagnetic reversals and excursions (Fig. 5) within cap carbonates (Trindade *et al*. 2003; T. Raub, pers. comm.), as well as lateral stratigraphic studies revealing complex interfingering relations of cap carbonate and siliciclastic intervals along the basin margin (Dyson & von der Borch 1994), suggest that cap deposition occurred on time scales approaching 1 Ma. These studies point to cap carbonates as a shelfal record of condensation of background carbonate sedimentation in the absence of siliciclastic deposition, which was pushed landward during post-glacial sea-level rise. Carbonate accumulation on flooding surfaces during transgression is common in Phanerozoic successions (Loutit *et al*. 1988) and may have been augmented by deep basinal alkalinity during deglaciation (Grotzinger & Knoll 1995; Ridgwell *et al*. 2003). These results are less consistent with non-uniformitarian models of rapid cap carbonate deposition during deglaciation that interpret the cap carbonates as the physical record of a non-steady state, large-scale reshuffling of carbon in the biosphere. Rather, they hint that most cap carbonate outcrops record condensation associated with the abrupt flooding in shallow intracratonic basins and not the higher resolution record of sea-level change available on basin margins, where a complex, cyclical sea-level history analogous to Phanerozoic deglaciation would be preserved.

The origin of the cap carbonate and its possible relation to changes in the carbon cycle during deglaciation are still open. At issue are the origin and mechanisms capable of producing the negative carbon isotope values common in each section, duration of cap carbonate deposition, unusual sedimentary structures, timing with respect to glacigenic deposits and stratigraphic relations at basin margins. Detailed facies, palaeomagnetic and diagenetic studies should help resolve this issue.

Chronology

Previous syntheses of Neoproterozoic glaciations (Hambrey & Harland 1981, 1985) relied heavily on Rb–Sr dates on shales, which are now known not to yield reliable ages. Indeed, estimates of the age of the Precambrian–Cambrian boundary varied widely (Harland *et al*. 1990) until the advent of U–Pb dating on zircons from tuffs (Bowring *et al*. 1993), but even now the field is critically short of reliable dates. Older literature often refers to the Vendian as a period encompassing Neoproterozoic glaciations, and a paradigm of two older Sturtian and two younger Varangian glacials was persistent (Kaufman *et al*. 1997). The common presence of only two glacial successions in any one section along with a consistent stratigraphic pattern of similar lithological and geochemical features reduced these intervals from four to two glacial horizons: a single Sturtian and Marinoan interval (Kennedy *et al*. 1998). U–Pb dates on zircons from acid igneous rocks, including tuffs, are the gold standard in terms of high accuracy and precision, with errors of a few million years by ion microprobe or laser-ablation inductively coupled plasma mass spectrometry (ICP-MS) and <1 Ma by thermal ionization mass spectrometry (TIMS) of samples from which U loss is eliminated by prior leaching procedures (Condon *et al*. 2005). The challenge is to find ash beds with datable zircons in geologically critical intervals. Re–Os dating of black (organic-rich) shales has provided an additional means of obtaining high-resolution ages, and with rigorous new sample preparation techniques, isochrons show errors akin to those for ion microprobe dates from zircons. Because black shales are more common than ash beds, this technique holds great promise for improving the general resolution of events and has provided the first dates from the Sturtian glacial interval in South and central Australia (Kendall *et al*. 2006) referred to above. In Figure 3a, we present only the most reliable dates. This strong filter still permits the reliable conclusion that there are not fewer than three

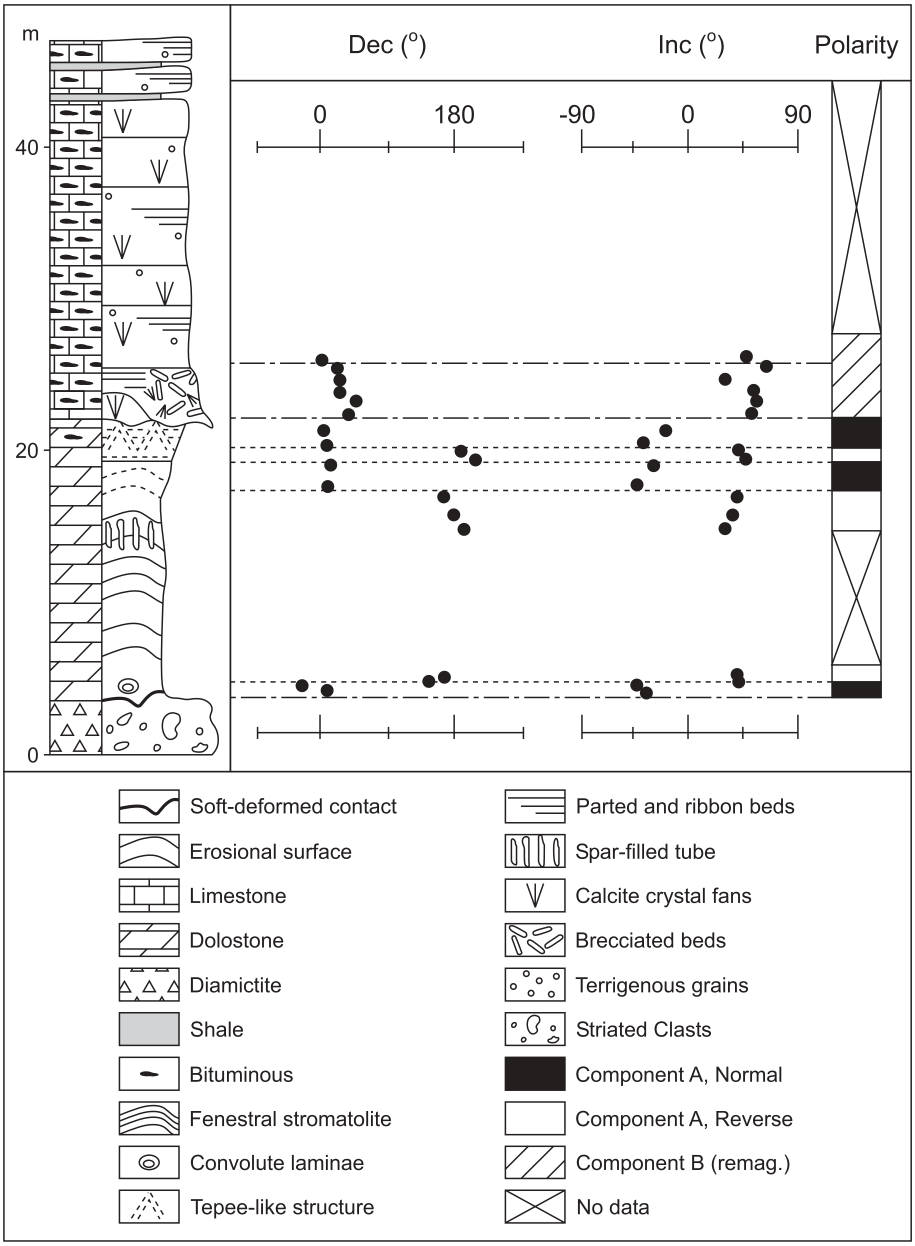

Fig. 5. Lithostratigraphy and magnetostratigraphy of the basal Mirassol d'Oeste Formation, a cap carbonate to the Puga glacial formation of the Amazon Craton (after Trindade *et al*. 2003). The presence of palaeomagnetic reversals is consistent with the cap representing condensed deposition.

Neoproterozoic glacial events or groups of glaciations. There is also an intriguingly close match of dates around the top of glacial deposits in Namibia and China argued to be Marinoan, but in detail a synchronous termination still remains to be demonstrated. The Hoffmann *et al*. (2004) Namibian age of 635.5 ± 1.2 Ma was obtained from an ash bed some 35 m below the top of a glaciomarine unit capped by dolomite and 140 m above the base of the intercalated glacial and volcanic facies. Condon *et al*. (2005) obtained their age of 635 ± 0.6 Ma from an ash horizon 2.3 m above the base of the cap dolomite in the Doushantuo Formation of the Yangtze Platform, South China, with a further date 1.7–3.8 Ma younger 3 m higher in the dolomite.

Hoffman *et al*. (1998) argued for a minimum of several million years duration for (Ghaub) glaciation, based on models of post-rift basin subsidence backed by the qualitative observation that the thick transgressive deposits overlying glacial deposits demonstrated significant accommodation space generated by basin subsidence. Using a more basic basin subsidence argument, one could estimate the proportion of time, within the 750–580 Ma interval, during which glacial deposits formed. In principle, this can be done by cumulating the thickness of glacial sediments and the overlying transgressive sediments, plus an estimate of the water depth of the deposits at the post-glacial maximum flooding surface, and expressing as a percentage of the total stratigraphic thickness within the glacial-prone era (750–580 Ma). A crude estimate on this basis is that glaciations occupied no more than 5–20% (8–35 Ma) of this era. Therefore, even the most conservative reading of the sparse information on the Sturtian shown in Figure 3a, with U–Pb dates indicating glaciation at least 40 Ma apart (667 and 712 Ma), is inconsistent with a single synchronous glacial event. If the oldest (Pb–Pb) and youngest (Re–Os) dates of >741 and 643 Ma are accepted, then it is certain that 'Sturtian' events must have been diachronous, but the older date (Frimmel *et al*. 1996) is in a terrain with more complex geological relationships.

The low error in U–Pb dating by TIMS provides the prospect of at least establishing the absolute time of an event, but it is a far more complicated stratigraphic problem to establish the duration of an event in a single local setting. An attempt to do this is the unpublished work by Bowring's group (quoted by Halverson 2006) on the 582 Ma Gaskiers glaciation in Newfoundland (Fig. 3c), which appears to be less than 2 Ma in duration. However, it would be just as valid to refer to this as a minimum duration, because the glacial record is notoriously incomplete. Glacial sedimentation is highly localized, ice-sheet advances commonly rework pre-existing land surfaces, and glacial sediments are often reworked by gravitational processes on slopes. Hence is also difficult to extrapolate the age of a single diamictite.

Another method of estimating the duration of glacial events has been suggested following the discovery of iridium enrichment, thought to be of extraterrestrial origin, within the base of cap carbonates on the eastern Congo Craton (Bodiselitsch *et al.* 2005). On the assumption that Ir was accumulated in static marine ice throughout the Marinoan glacial, and was abruptly released by melting at its termination, a duration of at least 3 and more probably 12 Ma accumulation (and hence glaciation) is proposed. However, both the assumptions of a static ice sheet and delivery as a uniform horizon within a transgressive, redeposited host sediment (the cap carbonate in this case was deposited through low-density turbidity flows) are questionable. Study of a wider assemblage of platinum group elements (PGE) in an analogous succession in NW Canada does not support their predominantly extraterrestrial origin (B. Peucker-Ehrenbrink, pers. comm.). Stratigraphic condensation and hydrogenous (i.e. seawater) enrichment associated with transgression is therefore a viable alternative mechanism for PGE concentrations.

Chronostratigraphy

In the Phanerozoic, most time-correlation is achieved by chronostratigraphy rather than radiometric chronology, using a combination of appropriate biostratigraphic and chemostratigraphic information calibrated with radiometric ages. However, prior to the Ediacaran Period, the preserved biotas (including cyanobacteria, acritarchs, and other algae) show little distinctive morphological variation over time, no better than that provided by changing stromatolitic and other distinctive carbonate facies, which indicate broad long-term co-evolution of sedimentary environments and biotas (Grotzinger & Knoll 1999). The most useful example is the absence of 'molar-tooth' limestone facies after the first evidence of Neoproterozoic glaciation (Shields 2002). Otherwise, chemostratigraphy, principally by $^{87}Sr/^{86}Sr$ and $\delta^{13}C$, more recently supplemented by $\delta^{34}S$, provides the basis for time-correlations. The correlation is based on an assumption of the precipitation of carbonate from a well-mixed and relatively isotopically homogeneous surface ocean and requires that significant carbon exchange does not happen subsequently during mineralogical stabilization to low-Mg calcite or dolomite, or during burial diagenesis. Carbon isotope chemostratigraphy has arguably become the principal means of correlation in the Neoproterozoic, with the recently assigned Global Stratotype and Stratigraphic Point (GSSP) for the Ediacaran Period partially based on the recognition of a global negative carbon isotope excursion. It is of slight concern that whereas negative carbon isotope trends are common in both the Phanerozoic and the Precambrian, it is only in the Precambrian, where independent means of establishing a synchronous origin with time control is difficult, that they are commonly interpreted as a record of seawater secular variation.

We are concerned about the quality control of many chemostratigraphic data. A key point is that the primary carbonate precipitates from ocean water were invariably metastable aragonite, vaterite, Mg-calcite or poorly crystalline dolomite, unlike the low-Mg calcite precipitates of organisms preferred for Phanerozoic studies. Stabilization occurs out of contact with the depositional water, and new carbonates can be created using alkalinity generated from decay of organic matter in the early diagenetic environment, decarboxylation in the deep burial environment, and meteoric fluids. In the case of Sr isotope ratios, the vast majority of Proterozoic carbonate samples are significantly more radiogenic compared with their original marine value (Shields & Veizer 2002), only formerly aragonitic Sr-rich (1000–3000 ppm) facies being generally reliable. Stratigraphic reproducibility of carbon isotope trends is often used as an argument for a primary marine origin resulting from secular variation of seawater change. It is argued that during stabilization the signatures do not change because carbonate acts as a relatively closed system and there is not sufficient dissolved carbon in stabilizing fluids to affect the isotope mass balance. This is justified by the modelling studies of alteration by meteoric water summarized by Jacobsen & Kaufman (1999). With logarithmically increasing degrees of recrystallization, first $\delta^{18}O$ values are reset, then Sr isotope ratios change as Sr contents are reduced and radiogenic Sr is introduced, and finally $\delta^{13}C$ can be lowered. Although the details of such models critically depend on the assumed water compositions, as well as the styles of alteration, this ranking of susceptibility to change is a good general guide. However, different stratigraphic units may have encountered completely different diagenetic systems, rendering a uniform assessment meaningless. For example, Fairchild *et al.* (1990) showed that two superimposed Neoproterozoic stromatolitic limestone formations from Mauritania had different histories. The lower, primarily Mg-calcite limestone was affected by marine diagenesis, which resulted in small negative shifts in $\delta^{13}C$ specific to different components in the same rock, whereas the upper, primarily aragonitic limestone was more strongly altered by meteoric water, which led to the production of a stratigraphic $\delta^{13}C$ anomaly that is a diagenetic artefact. Fe-bearing carbonates in general also have problems because, unless the depositional water was anoxic, they may have incorporated significant carbon generated by organic decomposition during early marine diagenesis. For example, Fairchild (1991) illustrated how $\delta^{13}C$ values in ferroan peritidal dolomites from eastern Greenland varied significantly over short stratigraphic distances. Early marine suboxic diagenesis also introduces Mn; the resulting relatively high Mn/Sr ratio should not of itself imply a strongly altered Sr isotope composition. Cathodoluminescence is sometimes used as a simple screening tool, but luminescence characteristics reflect both Mn and Fe contents and so the problem is not so readily solved. Studies of Quaternary marine carbonates where excellent independent time control between sections can be established demonstrate conclusively that alteration of marine carbonates is common and produces systematic carbon isotopic trends and negative absolute values similar to those taken as primary marine in origin (Gross & Tracey 1966; Swart & Eberli 2005). For these reasons, we recommend that petrogenetic studies be undertaken so that the nature and magnitude of secondary changes can be understood (and where quantifiable perhaps corrected for), rather than reducing the post-depositional history of entire successions to a single quantity termed 'diagenetic alteration'.

There are particular issues with dolomitization, as it requires an open system requiring hundreds to thousands of pore volumes of fluid to pass through the sedimentary rock, exchanging Ca with Mg (Land 1973). Dolomites tend to have lower Sr contents than limestones and rarely yield primary Sr isotope values. Although differences in $\delta^{18}O$ values of synsedimentary dolomites of different geological ages may in part reflect secular changes in seawater composition (Kasting *et al*. 2006), in general early diagenetic dolomite precipitates are metastable and will be expected to show post-depositional, probably multi-step re-equilibration behaviour (Frisia & Wenk 1994).

Sulphur isotope profiles and concentrations from carbonate-hosted sulphate may identify extremely dynamic changes in biogeochemical cycles, and abrupt shifts in the global oceanic oxygen and sulphate pool have been inferred (e.g. Hurtgen *et al*. 2002, 2006). However, there are large isotope and concentration fluctuations from one sample to the next and although this characteristic might be a reflection of low seawater S contents, it also raises issues of the variable fractionations associated with sulphate reduction, and subsequent changes during carbonate mineral stabilization from calcite to dolomite. More petrological information is needed before interpretations of secular changes and low sulphate contents in seawater can be confirmed.

We now illustrate the application of chemostratigraphy to stratigraphic successions. Figure 6a illustrates the NE Svalbard succession, from the work of Halverson *et al*. (2004) and Maloof *et al*. (2006), which adds significantly to previous studies. The glacial horizon at around 2200 m is preceded by negative $\delta^{13}C$ values, whereas the upper Wilsonbreen Formation at 2500m (illustrated in Fig. 2a) shows negative values only in the cap carbonate. In earlier work, negative carbon isotope values in Neoproterozoic carbonates were thought to be diagnostic indicators of the disturbance of the carbon cycle by glaciation (Kaufman *et al*. 1997), but this view has turned out to be untenable: such anomalies are polygenetic (Kaufman *et al*. 2006). For example, the broad anomaly at 450–750 m in the section of Figure 6a, named the 'Bitter Springs Stage' after its Australian correlate (Hill *et al*. 2000), is unconnected with glaciation (Maloof *et al*. 2006). Nevertheless, where cap carbonates are present, they show distinctively different patterns in older (Sturtian) and younger (Marinoan) examples in the same region (Fig. 6b), which Kennedy *et al*. (1998) proposed as one basis for distinguishing these glacial deposits. However, such differences may result from the timing of isotope excursions relative to carbonate deposition such that only portions of the isotope excursion are recorded in any one section. This carries the

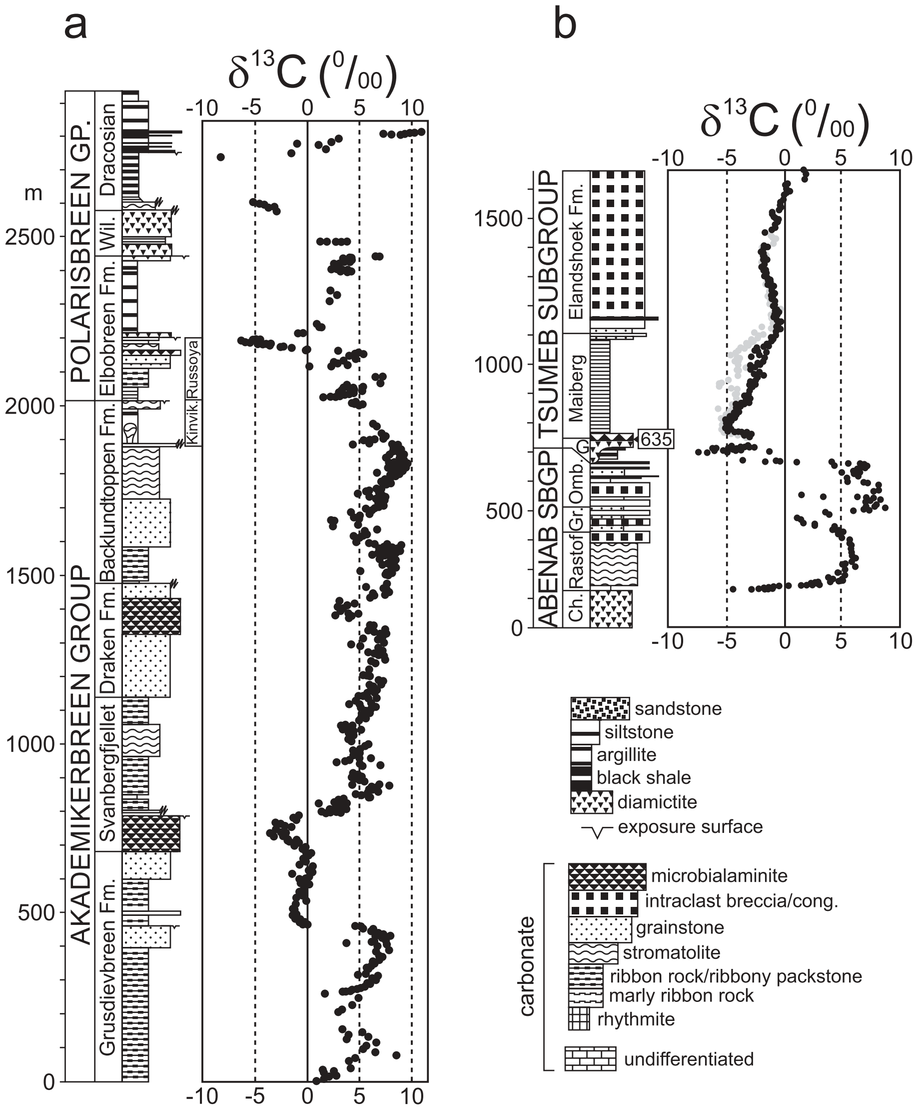

Fig. 6. Composite lithological and carbon isotope stratigraphies (after Halverson *et al*. 2004; Halverson 2006). (**a**) Akademikerbreen and Polarisbreen groups of NE Svalbard (Spitsbergen and Nordaustlandet). Glacial units are the thin unit (?Sturtian) in the Elbobreen Formation above the carbon isotope excursion at 2200 m, and the presumed Marinoan Wilsonbreen Formation (Wil.) at around 2500 m. The anomaly between 450 and 750 m (Bitter Springs Stage) coincides with palaeomagnetic changes attributed to an episode of true polar wandering (Maloof *et al*. 2006). (**b**) Section from Chuos Formation (Ch.; Sturtian) through to the Elandshoek Formation of the Otavi Group in northern Namibia, including two separate sections (stippled and filled circles) of the Tsumeb Subgroup. Gr., Gruis Fm.; Omb., Ombaatjie Fm.; G, Ghaub Fm. (the Marinoan glacial deposit, the top of which was dated to 635 Ma by Hoffmann *et al*. (2004)). The characteristically different carbon isotope profiles in the cap carbonate above the Chuos glacial deposits (increasing upwards) compared with the Ghaub glacial deposits (decreasing then increasing) should be noted; this was one of the criteria used by Kennedy *et al*. (1998) to define the Marinoan and Sturtian groups.

implication that the processes driving the isotope excursions are decoupled from the processes driving carbonate deposition, an issue of active research until the origin of both cap carbonates and the isotopic excursions is better understood.

Strongly negative $\delta^{13}C$ values beneath Marinoan glacial deposits in some sections in Namibia (Fig. 6b), NW Canada and South Australia (the Trezona anomaly), have been used to suggest an oceanic negative excursion preceding the glacial interval of up to −15‰ (Halverson *et al*. 2005). However, a shift to negative values is not present in all sections (Kennedy *et al*. 1998). Also, strong covariation between $\delta^{13}C$ and $\delta^{18}O$ (Schrag *et al*. 2002) and the presence of a karstified surface at the top of the Ombaatjie and Trezona Formations (McKirdy *et al*. 2001) raises some concern that these values record meteoric alteration. The presence of a global excursion was strengthened by correlation with a similar anomaly below the Elbobreen Formation glacial of Svalbard (at 2200 m in Fig. 6a) by Halverson *et al*. (2004) (although this correlation has now been changed because of doubts as to its Marinoan age; Halverson 2006). The correlatives of the Elbobreen glacial in eastern Greenland (a formerly contiguous basin, Fairchild & Hambrey 1995) show a similar deep anomaly in basinal facies that grade up into glacimarine facies, but laterally the basinal facies are capped by platform limestones with positive $\delta^{13}C$ signatures immediately below the glacial Ulvesø Formation. Hence Fairchild *et al*. (2000) proposed that this negative anomaly reflected a signature of a basinal environment. The study by Swart & Eberli (2005) of Cenozoic marine sediments demonstrates that basinal sediments can differ from shallow-water sediments for a variety of reasons, including differences in primary mineralogy, sediment-shedding from shallow-water environments, and contrasting evaporative and karstic alteration effects on the platform. Another issue is that pre-glacial anomalies might be variably removed by glacial erosion, and so will be more difficult to use for correlation.

A positive $\delta^{13}C$ anomaly between Sturtian and Marinoan deposits (Fig. 6b), strongest on inner shelf sections of the Otavi platform (Halverson *et al*. 2005), can be correlated with NW Canada (the Keele peak) and South Australia (Halverson 2006). Positive isotopic features are less likely to originate from diagenetic processes and so serve as much more robust points of correlation, particularly anomalously heavy values such as those that occur in the sub-Marinoan interval. A caveat is that non-marine settings could also yield heavy values (e.g. the top of Svalbard section of Fig. 6a, Fairchild & Spiro 1987).

Because of the diagenetic complexity of the carbon isotope results (particularly the negative values), and the difficulty of correlating a simple binary signal in the absence of detailed radiometric ages or biostratigraphy to provide an independent means of aligning peaks, we follow Melezhik *et al*. (2001) in holding that Sr isotope stratigraphy offers a more consistent approach to correlation, less fraught with the potential for circularity. The monotonic rise in marine Sr isotopic values through the Neoproterozoic (Fig. 7; Halverson *et al*. 2007) provides the best potential for unique correlations, although the effects of diagenesis, particularly with exchange from radiogenic clay minerals, can pose a significant problem in some successions. As shown by Kennedy *et al*. (1998) and Shields (1999), there is a consistent difference on the one hand between pre- and immediately post-Sturtian $^{87}Sr/^{86}Sr$ ratios of less than 0.7070, and on the other hand immediately post-Marinoan signatures of 0.7070–0.7075, rising rapidly to >0.709, which provides a criterion for differentiating these glacial intervals in ancient successions.

Palaeomagnetism and palaeogeography

Palaeogeography potentially provides a key to understanding drivers, extent, and hence intensity of the Cryogenian ice ages, yet it remains one of the most challenging parameters to pin down. Although sedimentary facies provide supporting evidence for continental reconstructions, the primary basis for understanding of palaeogeography at a given date has to be palaeomagnetism. The critical assumption is that the Earth has maintained a dominantly dipole magnetic field, oriented close to the Earth's axis of rotation, so that the inclination of the measured remnant magnetic vector is a simple function of palaeolatitude. The current consensus is that non-dipole (e.g. octupole) components of the field are subordinate (Evans 2000, 2006).

By combining information on apparent polar wander curves of Precambrian cratons with those provided by the distribution and

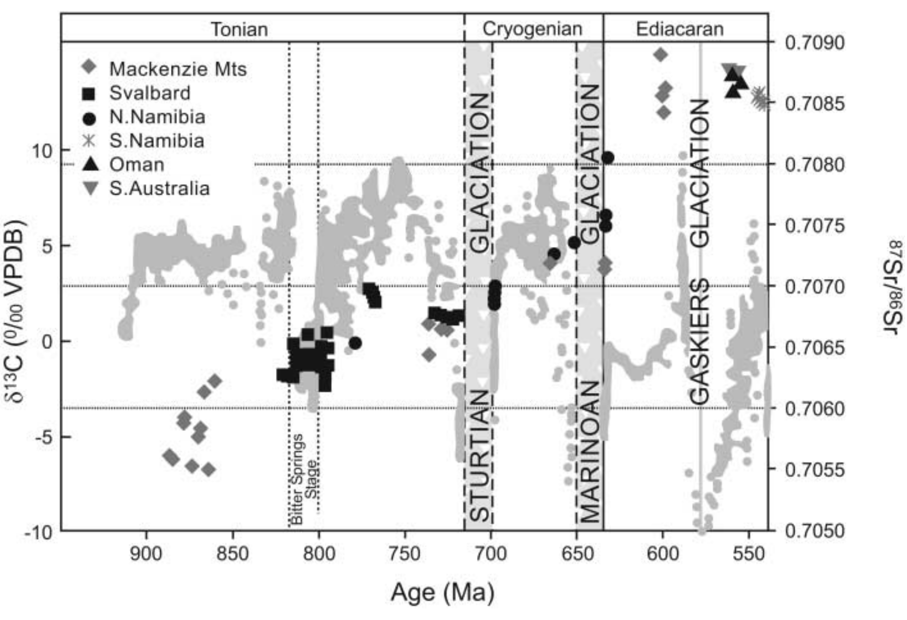

Fig. 7. Compilation from Halverson *et al*. (2007) of Sr isotope data from least-altered samples from several Neoproterozoic sections. Carbon isotope data are shown with faint symbols (geographical area not distinguished). No data are shown within the Sturtian and Marinoan deposits, which are given an arbitrary duration. The whole interval from the 'Bitter Springs Stage', constrained within a few tens of millions of years to 800 Ma (Halverson 2006), to the Ediacaran displays a long-term rise, with evidence of a weak pre-Sturtian decline in $^{87}Sr/^{86}Sr$ in Svalbard and Greenland (Fairchild *et al*. 2000). The registration of the Gaskiers glaciation with respect to the strong negative carbon isotope anomaly (Shuram–Wonoka anomaly) is not constrained radiometrically and other workers have placed it up to 30 Ma younger (Condon *et al*. 2005; Fike *et al*. 2006).

age of mobile belts, the existence of an early Neoproterozoic supercontinent (Rodinia) emerges (Dalziel 1997). During the Neoproterozoic, Rodinia split, and the rifted components (East and West Gondwana) had collided on their freeboard margins by the beginning of the Cambrian (Fig. 8a; Cawood 2005). The details of these events are very difficult to specify because of a lack of age constraints and because of the varied quality of palaeomagnetic data. An extreme parsimonious approach is to use only the highest quality palaeomagnetic data from multiple localities, precisely (U–Pb) dated from volcanic, shallow intrusions and associated rocks, to provide key palaeomagnetic poles (Buchan *et al*. 2001). On this basis, both Laurentia and Australia were equatorial around 750 Ma, although their relative longitudinal positions are unconstrained (Fig. 8b). By accommodating other data from several cratons, a broader picture of a rifted Rodinia at 750 Ma emerges (Fig. 8c; Torsvik 2003), which contrasts starkly with the Phanerozoic norm of glacial eras starting on a polar continent. Although the 750 Ma configuration is commonly used to understand forcing factors for Sturtian glaciation (e.g. Hoffman & Schrag 2002), the appropriate palaeogeography for later events is much more conjectural because of limited reliable radiometric ages and so we do not illustrate a reconstruction in this review. Such is the uncertainty that some modelling work (e.g. Pollard & Kasting 2004) has resorted to the 540 Ma palaeogeography, with cratons stretching from equator to South Pole, as a surrogate for the Marinoan glaciation. We are still a long way from being able to assess specific examples of opening and closing of oceanic gateways in the Proterozoic as controls on the development of glaciations as they were in the Phanerozoic (Smith & Pickering 2003).

Direct determinations of palaeolatitude from glacial or adjacent formations have produced a dominance of low palaeolatitudinal results, but the acceptability bar for data quality has risen progressively as the discipline of palaeomagnetism has matured and procedures for distinguishing primary from secondary magnetizations of different ages have improved. Although early results were invalid (Evans 2000), an equatorial palaeolatitudinal result for glacial deposition has always been on the table since 1959, a constant thorn in the side of models of rapid continental drift over the poles to explain Neoproterozoic glaciation (Meert & van der Voo 1994). A highlight has been the work on the south Australian Elatina Formation, a Marinoan glacigenic formation that also contains many sorted siliciclastic sediments including tidal rhythmites (Williams 2000). Through the work of Embleton & Williams (1986), Schmidt & Williams (1995) and Sohl *et al*. (1999) progressively more diverse and rigorously tested data have been obtained to support low palaeolatitudes for glaciation. Sohl *et al*. (1999) made a breakthrough in demonstrating repeated reversals of the palaeomagnetic field and hence deposition of the Elatina Formation over $>10^5$ 10^7 years as well as estimating palaeolatitude at $8 \pm 6°$ (95% confidence limits) at the onset of glaciation. The deglacial context, including the basal Ediacaran GSSP, is being clarified by the detailed work of Raub *et al*. (2007). Reliable repeated magnetic reversals have now also been demonstrated from the dolomite capping the late Neoproterozoic Puga glacial of the Amazon Craton (Fig. 5; Trindade *et al*. 2003; $22° +6°/-5°$ palaeolatitudes).

A controversial, but potentially important process for explaining the initial onset of glaciation in the Neoproterozoic is rapid true polar wander (TPW), a small component of which is thought to characterize plate movements even in the last 200 Ma (Besse & Courtillot 2002). Both in the period prior to 750 Ma and in the early Cambrian (Evans 2003; Li *et al*. 2004; Maloof *et al*. 2006), a co-ordinated movement of cratons faster than known Phanerozoic rates of continental drift has been evoked. The apparent TPW events are attributed to a relative movement of the entire crust and mantle with respect to the outer core, tending to bring a prolate axis (aligned with an upwelling plume located beneath a supercontinent) to equatorial regions, where continental fragmentation occurs (Evans 2003). Li *et al*. (2004) specifically argued for a 90° anticlockwise rotation of a pole-to-equator Rodinia between 800 and 750 Ma about an axis near Greenland to produce the equator-straddling configuration of reconstructions like that of Figure 8c, a palaeogeography conducive to drawdown of atmospheric CO_2 and the development of glaciation (Kirschvink 1992).

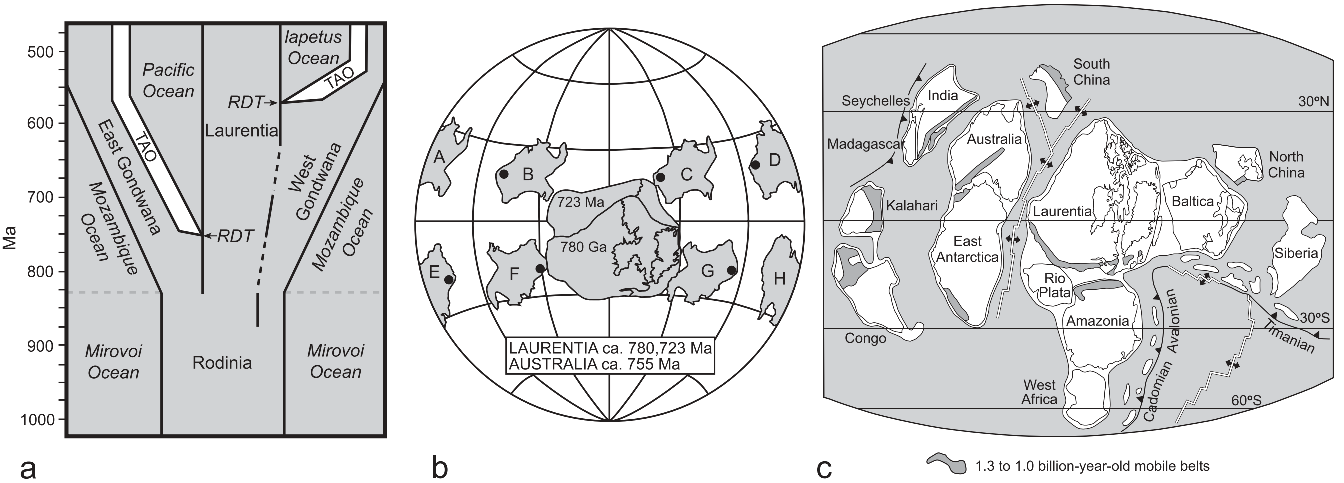

Fig. 8. Palaeogeographies. (**a**) Schematic diagram illustrating the fragmentation of supercontinent Rodinia and the subsequent collision of East and West Gondwana by 550 Ma (after Cawood 2005). TAO, Terra Australis Orogen (a complex evolving margin of Gondwana); RDT, rift-to-drift transition. (**b**) Use of only key palaeomagnetic poles to make a parsimonious reconstruction of Laurentia at 780 and 723 Ma together with permissible (A–H) locations of Australia relative to Laurentia (Buchan *et al*. 2001). (**c**) Example of a 750 Ma reconstruction illustrating a fragmenting Rodinia with putative plate boundaries. Palaeomagnetic data at 750 Ma are available only for the cratons of Congo, India, Australia, Laurentia and Baltica (Torsvik 2003).

Conceptual models for Neoproterozoic glaciation (Fig. 1)

Slushball Earth

In the introduction, we described Slushball Earth as a pragmatic synthesis, but it was not so initially. At a time when continental drift was only just becoming the respected norm, Brian Harland actively promoted the idea of a global glaciation (Harland 1964) based on palaeomagnetic results implying equatorial palaeolatitudes for Neoproterozoic glacial deposits from Greenland and northern Norway. Many scientists, including sedimentologists inclined to interpret diamictites as mass flows, saw this as an extreme view, polemically argued, and Harland was clearly stung by the criticism (Harland & Herod 1975). Indeed, the initial palaeomagnetic data were later found to be invalid, but Harland was in any case convinced from the widespread occurrence of glacial deposits. We emphasize that Harland's concept was a Slushball Earth not a Snowball because Harland & Rudwick (1964) made clear that open water would have remained in equatorial regions. In a paper (Harland 2007) prepared in the year of his death (2003), Harland expressed the wish to reclaim the Snowball title for his own (unchanged) views, referring to the Hoffman *et al*. (1998) theory instead as Iceball Earth (others have likewise referred to the hard Snowball, e.g. Pierrehumbert 2005). However, here we use the term Slushball Earth, a phrase coined by Schrag & Hoffman (2001) to refer to a climate model solution of Hyde *et al*. (2000) close to Harland's conception.

The Slushball solution accommodates the following propositions (Fig. 1).

(1) There is sufficient evidence from palaeomagnetism (Evans 2000), sedimentary facies (Fairchild 1993) and distribution of glacial sediments (Hambrey & Harland 1985) to accept that glaciers extended to tropical palaeolatitudes at sea level.

(2) The wide extent of glaciation, coupled with the occurrence of only up to three major glacial units in any one succession, implies that glaciations were few and discrete, and hence impacts (e.g. sea-level change or disturbance of the C cycle as manifested by $\delta^{13}C$ anomalies) may be correlatable globally (Harland 1964; Knoll *et al*. 1986; Kennedy *et al*. 1998; Halverson 2006). A caveat is that the current consensus is that neither a negative $\delta^{13}C$ isotope anomaly *per se*, nor the presence of a glacial unit in a formation of unknown palaeolatitude, would now be regarded as evidence for a near-global glaciation at the time of deposition.

(3) Facies analysis of the glacial intervals, tested against modern analogues, implies a hydrologically active glaciation at sea level; in some cases glacial deposits demonstrably grade laterally, or over time, into open-marine sediments (Eyles & Eyles 1983; Leather *et al*. 2002).

As stated, the Slushball Earth's weakness as an intellectual framework is that it does not describe unique Earth System behaviour related to specified forcing factors except for the requirements placed on the Earth System by the extreme state of tropical ice at sea level. Hence, apart from the obvious requirement that new radiometric dates should cluster around a small number of age ranges, the Slushball hypothesis, which has been arrived at inductively, does not readily produce predictions for future testing. Rather, it is strengthened by negative tests of other hypotheses. For example, the original Snowball hypothesis did not allow for a role of methane release in facilitating deglaciation (Kennedy *et al*. 2001*a*), which led to a successful search for contemporary methane seeps (Jiang *et al*. 2003).

Zipper-Rift Earth

An intellectual tradition critical of evidence for low-latitude Proterozoic glaciation, developed for example from the work of Crowell (1957) and Schermerhorn (1974), has been enhanced by Nick Eyles, who has added to the sedimentological perspective a broad understanding of modern glacial facies. Eyles (1993) emphasized the tectonic setting of glacial and alleged glacial strata, and argued for a regional tectonic–adiabatic control on the occurrence of glacigenic sediments (Fig. 9). Eyles &

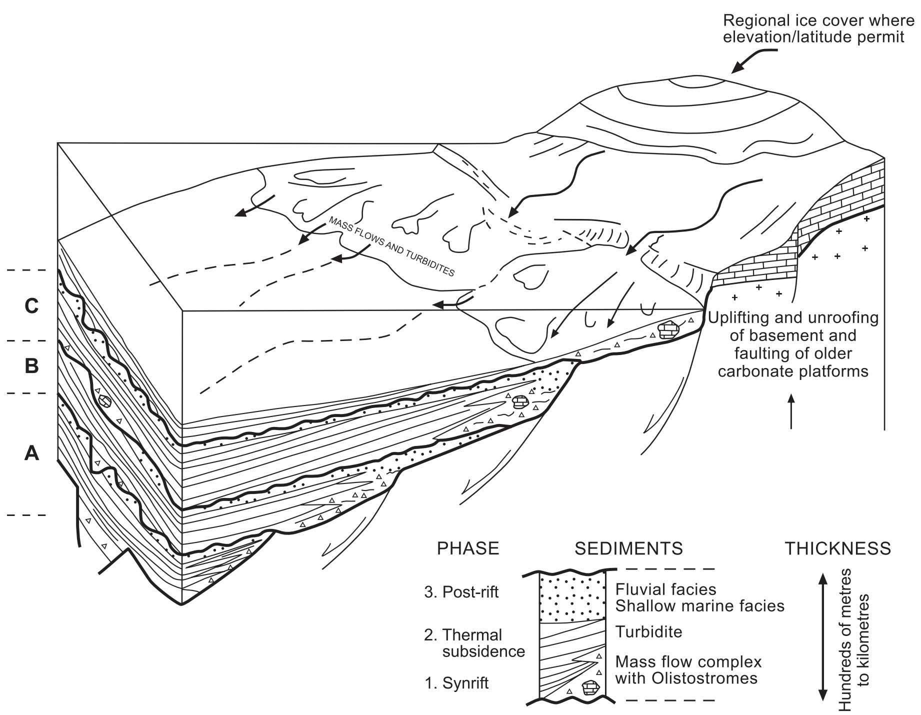

Fig. 9. Formation of tectono-stratigraphic successions along a rifted basin margin in which diamictite sedimentation is regarded as the response to a phase of uplift and, in different cases, may or may not be associated with glaciation (Eyles & Januszczak 2004).

Januszczak (2004) then developed the term 'Zipper-Rift' (Fig. 1) to refer to the first-order control of diachronous rifting of the supercontinent Rodinia on the occurrence of glaciers on uplifted rift-shoulders, and the preservation of glacial sediments in rift basins (Young 1984). Eyles & Januszczak (2004) accepted modern sedimentological analogues for siliciclastic facies, but were sceptical of evidence of low-latitude glaciation from palaeomagnetic or other facies evidence. They emphasized that the presence of few, time-limited glaciations has not been demonstrated by radiometric dating and discounted attempts at global chemostratigraphy linked to $\delta^{13}C$ anomalies.

Like the High-tilt and Snowball models, Zipper-Rift Earth is argued for polemically by its protagonists. Proponents of global glaciation were bracketed with earlier catastrophic traditions stemming back to Norse legends by Eyles & Januszczak (2004), although to their credit they accounted for many of the geological observations in their review. Nevertheless, their dismissal of the significance of cap carbonates as integral parts of Neoproterozoic glacial cycles, by appealing to clastic redeposition, or major time gaps separating them from glacial deposition, does not account well for a wealth of published evidence. Likewise, more palaeomagnetic evidence of low palaeolatitudes associated with glaciation is accumulating as discussed above. The importance of this work has been to emphasize the tectonic context of evidence of glaciation, and representatives of the 'Sturtian' glaciation in particular appear to be diachronous, as predicted by Zipper-Rift Earth.

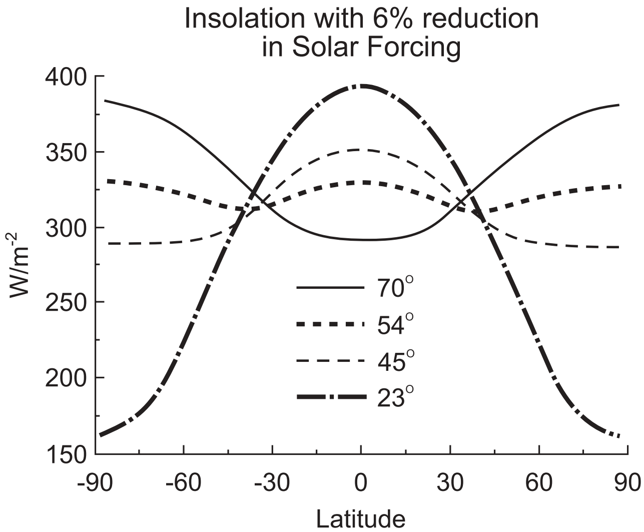

Fig. 10. Mean annual insolation received at different latitudes (zonally averaged) given varying obliquity (tilt) angles of the Earth's spin axis to the normal to the orbital plane (after Jenkins 2004*b*). Current tilt displays cyclic (Milankovitch) variations within the range 22–24°. As pointed out by Williams (1975), a tilt of more than 54° results in higher annual heat receipts at the poles than the equator.

High-tilt Earth

George Williams has made a number of important contributions to sedimentary geology, cyclostratigraphy and planetary dynamics, in addition to his promulgation over 35 years of what we term the High-tilt model. This proposes that Neoproterozoic glaciation was a phenomenon preferentially developed at low palaeolatitudes because of high obliquity; that is, an enhanced tilt of the Earth's spin axis in relation to the Earth's orbital plane (e.g. Williams 1972, 1975, 2000; Williams & Schmidt 2004). If the Earth's obliquity is greater than 54° (compared with the modern range of 22–24° over 41 ka cycles), more heat is received annually at the poles than the equator, tipping the balance towards preferential low-latitude glaciation (Figs 1 and 10, Jenkins 2004*b*). An important accompanying effect is a greatly enhanced seasonality of temperatures. Williams' key arguments are: (1) the palaeomagnetic and facies evidence for low-latitude glaciations in contrast to the under-representation of high-latitude ones; (2) evidence of large annual temperature changes in sediments known to be in equatorial latitudes. Evans (2000) concluded that the palaeomagnetic database was not yet good enough to distinguish between a uniform distribution of glacial deposits and a preferential low-latitude distribution. The model has not extended into the possible biogeochemical consequences; it may be consistent with the evidence that the Snowball and Slushball models have in common (Fig. 1), but it does not predict them.

We referred above to the work of Williams in obtaining palaeomagnetic evidence for low-latitude glaciation in southern Australia (from Embleton & Williams 1986, onwards) which, following subsequent work, was given the highest probability rank in the palaeomagnetic compilation of Evans (2000). In his early presentation (Williams 1975), a variety of arguments for seasonal temperature change were made, some of which, such as reddening of tills, were erroneous (Fairchild & Hambrey 1984), or on uncertain time scales. The later findings of periglacial phenomena such as sand wedges and a block field in South Australia (Williams & Tonkin 1985) are more compelling, as the argument has been made that they require strong temperature forcing that could only be accomplished on the annual scale, rather than the short-lived temperature fluctuations that give rise to weak periglacial phenomena around equatorial mountain glaciers today. This viewpoint has been countered by Maloof *et al*. (2002), who showed that material properties are important in the depth of development of patterned ground wedge-structures and argued that diurnal temperature cycling could generate these periglacial phenomena. Pierrehumbert (2005) also picked up on the point that, in modern high-latitude areas, the specific forcing that generates seasonal contraction arises from rapid cooling from early winter synoptic weather systems, and so the issue is whether such systems will occur at the low latitudes of South Australia in the Neoproterozoic.

Although these views, taken in isolation, are balanced, other evidence argues against the High-tilt Earth. The most widely discussed argument is that it is difficult to change the Earth's obliquity over time given that, unlike some other planets, change is limited by the coupling of the Earth–Moon System. Williams (1993) argued for a reduction in obliquity to values close to the present-day one by 430 Ma, when there is independent evidence of the tilt angle. However, planetary dynamicists do not find any currently acceptable mechanism for this to have occurred (Levrard & Laskar 2003). Evans (2006) also found that the palaeomagnetic latitudes of Proterozoic evaporites were not consistent with high obliquity. Another, less tangible issue, is that high obliquity and the accompanying extreme seasonality ought to be accompanied by sedimentological evidence of different kinds of annual phenomena than are found at the present day not only during, but also before and after glaciation, but we judge that such problematic structures have not been identified. Finally, it should be pointed out that that the evidence for seasonality at low palaeolatitudes is much stronger that that for preferential low-latitude glaciation. Hence, a more robust version of

Williams' hypothesis would be for a moderate, rather than large increase in tilt.

Snowball Earth

The palaeomagnetist Joseph Kirschvink applied the term 'snowball' to refer to an ice-covered Earth during Neoproterozoic glaciation (Kirschvink 1992). A more highly developed model, termed the Snowball Earth hypothesis, was subsequently developed by Paul Hoffman and Dan Schrag, reflecting their combined expertise in Proterozoic geology and oceanic modelling respectively, and leaning on the chemostratigraphic experience of Jay Kaufman (Hoffman *et al*. 1998; Hoffman & Schrag 2000, 2002).

An attraction of Snowball Earth is the way it attempts an integrated Earth System science perspective, building on developments in geology and theoretical climatology, allowing scientists from a wide variety of backgrounds to test its implications. One starting point was the development of simple energy-balance models by climatologists such as Budyko (1969), which allow the calculation of the effects of albedo and meridional (poleward) heat transport in converting the distribution of incoming shortwave radiation into observed climatic belts. Budyko (1969) described the consequences of a positive feedback between the growth of ice sheets with high albedo, and temperature. During growth of an ice sheet, the increased reflectivity of the surface, leading to reduced ground radiation of heat, would lead to further coverage of ice; Budyko (1969) found that once ice reached a critical latitude, the system became highly nonlinear and global glaciation rapidly ensued. This would now be described as a climatological discontinuity or bifurcation: a runaway glaciation, where the positive ice–albedo effect is not countered by negative feedbacks. However, Walker *et al*. (1981) described such a negative feedback in the context of box-modelling of long-term cycling of CO_2 ultimately derived from volcanic outgassing. They noted that chemical weathering of silicates, which removes atmospheric CO_2, is temperature-dependent, and so would have slowed down as glaciation was initiated. When Marshall *et al*. (1988) incorporated this feedback into their energy-balance model, they found that it prevented global glaciation, but still permitted cold climates in the case where continents were clustered around the equator, as chemical weathering rates are high in the moist tropics. Caldeira & Kasting (1992) corrected some aspects of Marshall *et al*.'s model and showed using energy-balance modelling that if ice sheets and sea ice spread beyond a critical latitude of 30°, runaway global glaciation ensued; they also calculated that CO_2 would have to have accumulated to a pressure of 0.12 bar (at present solar radiation values) to terminate glaciation through a greenhouse warming effect.

Hoffman & Schrag (2002) further developed this approach by expressing the albedo effects diagrammatically, based on energy balance model results showing three stable climate states for Earth. These are shown as continuous lines in Figure 11a: ice-free, partly ice-covered, and ice-covered. A reduction in energy absorption by atmospheric greenhouse gases such as CO_2 and/or other means for reducing the flux of solar radiation causes a lowering of temperature from point 1 to point 2 on the partly ice-covered branch as ice extends to progressively lower latitudes. A discontinuity is reached and the albedo effects jump the system to the ice-covered, Snowball state at point 3 with a surface mean temperature of around −50 °C (Fig. 11). This in turn leads to a minimum of mass and energy exchange between atmosphere and oceans, a drastically reduced hydrological cycle and a cessation of continental chemical weathering. This state permits, over the following 3–30 Ma, a gradual accumulation of volcanically derived greenhouse gases in the atmosphere, leading to gradual warming and intensification of the hydrological cycle. Another threshold (point 4 to point 5) is crossed when the increasingly warm atmosphere drives the ice–albedo effect into reverse and leads to deglaciation and global cap carbonate formation resulting from the accumulation of CO_2 in the atmosphere from the absence of a weathering sink during the Snowball event (point 5); enhanced rates of silicate weathering consume the excess atmospheric CO_2, which is expelled into the oceans as alkalinity

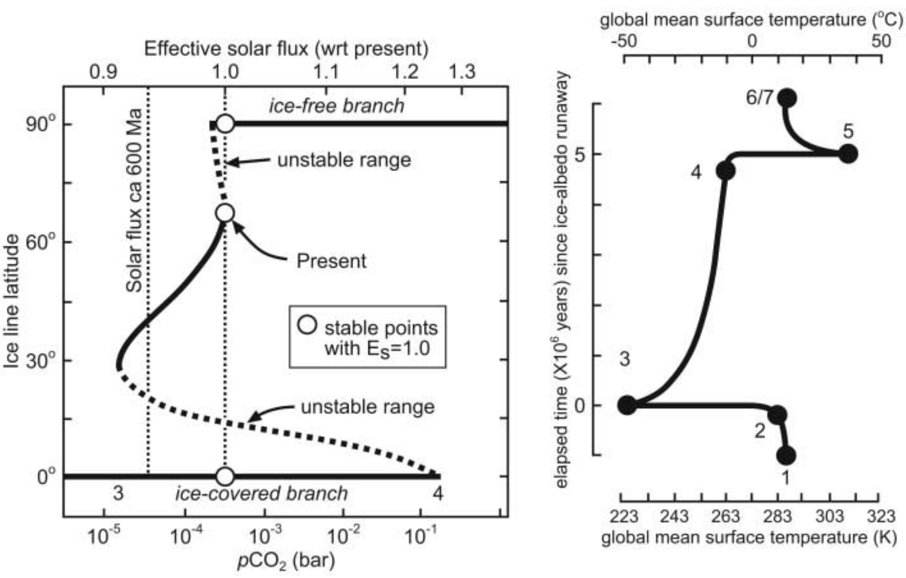

Fig. 11. Changes in Earth state envisaged by the Snowball Earth model (after Hoffman & Schrag 2002) derived from energy-balance modelling based on Caldeira & Kasting (1992) and Ikeda & Tajika (1999) and using an albedo of 0.6 for ice cover and present-day meridional heat transport. The diagrams are intended to indicate behaviour qualitatively, rather than give quantitative predictions. A Snowball Earth event is represented by numbers 1–7. In (**a**) continuous lines represent stable ice-free, partly ice-covered, and ice-covered states of the climate system, shown as the lower latitudinal limit of sea ice as a function of E_s (solar fluxes ratioed to present-day flux). The PCO_2 values on the lower *x*-axis are those that apply for a present-day solar flux ($E_s = 1$). At 600 Ma, the relevant solar flux is 0.94 and the same behaviour will be shown as at the present day, but at systematically higher PCO_2 values to balance the lower solar flux. (**b**) pattern of temperature change: results and time scale are indicative.

and precipitates as the cap carbonate at high surface temperatures (point 6). The system then reverts to the initial condition (point 7). The Snowball model thus makes strong predictions about stratigraphic development and rates of deposition of glacial and post-glacial deposits and the effects on life and geochemical cycles.

A novel aspect introduced by Kirschvink (1992) was the link between a global oceanic ice cover at a specific time in Earth history, the generation of bottom-water anoxia in the absence of wind-mixing, and the association of Banded Iron Formation with glacial periods. Hoffman *et al*. (1998) blended all these ideas, together with a new concept of how glaciation linked to a disturbance of the carbon cycle. This arose from new chemostratigraphic observations in Namibia showing a fall in $\delta^{13}C$ value prior to glaciation, as well as the presence of the isotopically light cap carbonate (Fig. 6b). Hoffman *et al*. inferred that $\delta^{13}C$ values remained negative throughout the ice age and proposed a global shutdown of productivity brought about by an ocean-scale ice sheet. They further considered that the carbonate caps formed globally as the Earth System responded to the enormous build-up of CO_2 with the shutdown of the hydrological cycle and the chemical weathering sink on land. During deglaciation, intense chemical weathering of silicates transferred carbonate alkalinity to the oceans, resulting in a rapid precipitation of carbonate blanketing marine environments.

The Snowball Earth hypothesis of Hoffman *et al*. (1998) made definite predictions testable in the geological record based on the energy balance models evoking the catastrophic effects of the albedo feedback. Subsequent to the initial publication in 1998, however, the predictions became less specific as difficulties in the original conception became apparent. Hoffman & Schrag (2002) qualified the hypothesis and simple falsification of some of the initial, seemingly supportive, lines of evidence was no longer possible. One change was to withdraw the interpretation that the $\delta^{13}C$ anomaly resulted from a shutdown in productivity, Kennedy *et al*. (2001*b*) having shown normal carbon isotopic values in glacial intervals. Instead, Schrag *et al*. (2002) and Higgins & Schrag (2003) related the carbon anomaly to hypothesized pre-glacial methane release together with post-glacial fractionation effects driven by temperature and carbon saturation. Hoffman & Schrag also recognized that alkalinity release from silicate weathering was not likely to be rapid enough to account for cap carbonates, referring to carbonate weathering instead, but because carbonate weathering does not permanently remove CO_2 from the atmosphere, this decouples the cap carbonate and the carbon isotope anomaly from the recovery to more normal atmospheric CO_2 levels.

Quantitative modelling

As introduced in the previous section, modelling approaches are diverse and, because the Neoproterozoic world was so different from that today, have played an important role in setting an agenda for what must first be explained (e.g. the implications of equatorial ice sheets at sea level). Mass-balance models are used, for example, to model the rates of deposition of oxidized and reduced forms of isotopic species. Biogeochemical models simulate the coupling of different elemental cycles to each other and to climate. Climate models range in complexity from energy-balance models (EBMs) that focus on the latitudinal partitioning of energy inputs and outputs to full general circulation models (GCMs). Discrete modules dealing with specific processes, such as ice-sheet behaviour, or certain biogeochemical cycles can be run separately to provide input parameters, or be coupled to the climate model. A useful role is played by intermediate complexity models that allow a larger range of simulations than in the computationally intensive GCMs. The applicability of models is limited both by reliable geological information and by computational constraints, but considerable progress has been made over the past decade on both fronts.

In this part of the paper, we first examine the insights that have been gained by modelling of physical factors affecting extreme climates: such climate models usually take atmospheric composition as a given. We then show the results of simulation models have helped identify the main tectonic and biogeochemical system drivers and feedbacks that influence atmospheric composition and, in turn, glaciation.

Climate models of extreme glaciation

Pierrehumbert (2005) summarized the attraction of the problem to modellers both as a fundamental test of modelling skill and also in terms of addressing problems of life survival on Earth and other potentially habitable planets: ‘The passage through a Neoproterozoic hard snowball state would be so remarkably interesting, if true, that it repays further study even though some might assign a low probability to such an event having actually happened’. Thus, publication of the paper by Hoffman *et al*. (1998) has been followed by rapid development of climate modelling work, the field being characterized by many ‘leapfrogging’ studies that modify earlier conclusions.

Two critical factors that drive the Earth to extreme glaciation are lower greenhouse forcing and higher surface albedos. Greenhouse forcings are normally prescribed inputs to a simulation and expressed as equivalent values of PCO_2 (water vapour and methane are implicit). The key role of the greenhouse gases is to absorb outgoing long-wavelength radiation from the Earth’s surface, which today results in a mean temperature 30 °C higher than would be the case in the absence of an atmosphere. To attain the same temperature as today, greenhouse gas forcings would have needed to have been slightly higher than at present to compensate for a 6% lower solar radiation in the Neoproterozoic. Different models yield solutions ranging from 90 to 1800 ppm (Poulsen & Jacob 2004) for the critically low PCO_2 value that would lead to global sea-ice cover (compared with 180 and 280 ppm respectively for Quaternary glacial and interglacial periods). Variations in the treatment of water vapour, clouds, wind-driven circulation and ice albedo all contribute to these differences (Pierrehumbert 2002; Poulsen & Jacob 2004). The high albedo of snow and ice provides the strongest positive feedback mechanism driving the Earth into glaciation, but various reseaerchers have used different albedo values, which have had major impacts on their modelled outcomes (Warren *et al*. 2002; Pierrehumbert 2005). The runaway ice–albedo effect is strong in various model types, and some models suggest a consequent difficulty in maintaining a Slushball Earth over long (10^5–10^7 years) timeframes (Donnadieu *et al*. 2003).

An early Slushball solution was provided by Hyde *et al*. (2000). Initially, by using an ice-sheet model coupled to an EBM, which had been successfully calibrated on younger glacial periods, they obtained a runaway Snowball state with PCO_2 $\leq$0.5 times present atmospheric levels (PAL), otherwise ice at sea level reached only 40° latitude. However, when they used the ice-sheet results from such simulations as input to the GENESIS2 GCM, a Slushball solution with sea ice to 25° latitude was stable at PCO_2 at 2.5 times PAL. This difference from the EBM work was attributed to two factors: the GCM-produced reduction in cloudiness (and hence albedo) in the tropics, and ocean circulation-limited sea-ice distribution. This study (see also Baum & Crowley 2001; Peltier *et al*. 2004) remains one of the few that have attempted to model ice-sheet behaviour, but the GCM work suffers from unconstrained palaeogeography and a parameterized ocean heat transport rather than dynamical ocean circulation.

The modelled Snowball climate state, with a mean temperature around −50 °C, displays some remarkable features (Pierrehumbert 2004, 2005). Seasonal temperatures closely reflect the input of solar radiation as there is relatively little atmospheric heat transport; hence seasonality is enhanced compared with today, and the diurnal temperature cycle is also very strong, allowing daily runoff to feed lakes (Pierrehumbert 2005). A weak hydrological cycle is present, which results in millimetres to centimetres of sublimation and precipitation annually (Pierrehumbert 2002; Goodman 2006). This is sufficient over periods $>10^5$ years to build up substantial ice sheets, which, like the modern East Antarctica ice sheet, may have wet bases and develop distinct rapidly moving zones (ice streams) in which erosion and deposition may be focused (Donnadieu *et al*. 2003, based on an ice-sheet model driven by atmospheric GCM results). Conversely, low-elevation continental interiors at low latitudes would become ice-free (Pierrehumbert 2004). The marine realm would see the accumulation of thick sea ice, both by snow deposition and by freezing-on of seawater from below. Once this attained a thickness of 50–100 m, it would deform under its own weight, becoming a sea glacier (Warren *et al*. 2002). Goodman & Pierrehumbert (2003) referred to sea glaciers' capability of significant erosion and sediment transport, which could account for glacial diamictites limited to locally sourced carbonate debris. A recent modelling study of sea glaciers under Snowball conditions using a dynamic sea-ice model coupled to an EBM (Goodman 2006) demonstrates that their flow would lead to thick ice nearly everywhere (Fig. 12). However, Pollard & Kasting (2005) pointed out that thin ice, within which normal marine planktonic life might survive, could be associated with continental embayments.

A rapid deglaciation of Snowball Earth as the ice–albedo effect goes into reverse (Fig. 11) is a general feature of climate model results. However, a $P\text{CO}_2$ level of 0.12 atm to deglaciate a frozen planet (Caldeira & Kasting 1992) has been taken rather too literally in the geological literature. First, this value applied to present-day solar luminosity, so the threshold would have been higher in the Neoproterozoic. Second, a more sophisticated approach leads to a Snowball Earth still 30 °C short of the threshold to deglaciate at 0.2 atm, the limit of applicable radiation physics (Pierrehumbert 2004, 2005). Even the lower CO_2 threshold would take 28 Ma to develop (at present outgassing rates) if two-thirds of outgassed CO_2 had accumulated in the oceans (via cracks and patches of open water) as assumed by Higgins & Schrag (2003). Very high $P\text{CO}_2$ would be even harder to reach if sea-floor weathering of basalts (Brady & Gislason 1997) or clays were to be taken into account. On the other hand, much lower levels of CO_2 (EBM–ice-sheet model studies suggest four times PAL, Crowley *et al*. 2001) would be needed to remove tropical ice at sea level from a Slushball Earth. Crowley *et al*. (2001) and Peltier *et al*. (2004) found a hysteric behaviour that permitted variations in intensity of a Slushball state over long periods (Fig. 13). Peltier *et al*. (2004) showed from related preliminary short GCM studies that ocean dynamics were important in this respect, but also proposed that biogeochemical feedbacks could play a role (see next section).

Important insights from Snowball modelling studies that may apply to some extent to Slushball Earth include the behaviour of

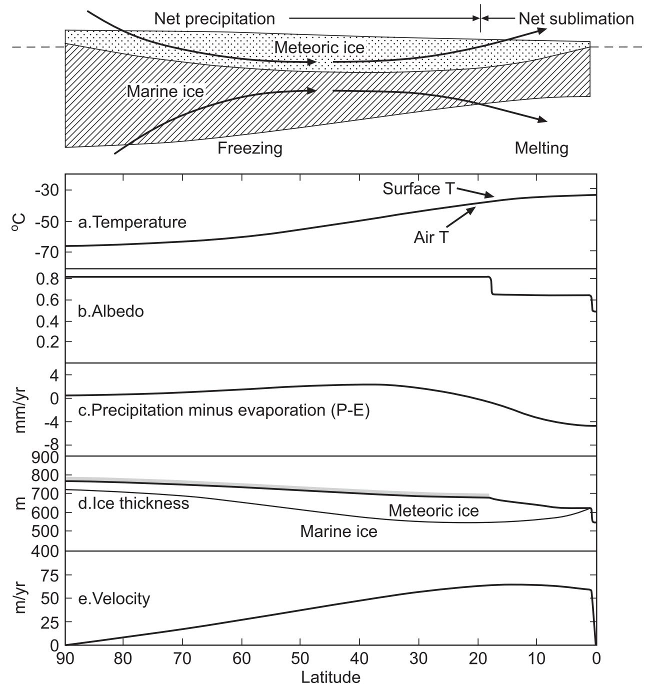

Fig. 12. Behaviour of an idealized zonally symmetrical sea glacier (after Goodman 2006). A weak hydrological cycle leads to sublimation in the tropics and deposition of snow in higher latitudes. Also, there is freeze-on of seawater at the base of the sea glacier at higher latitudes. These processes are compensated for by equatorwards flow of the sea glacier with a very narrow strip of thinner ice at the equator.

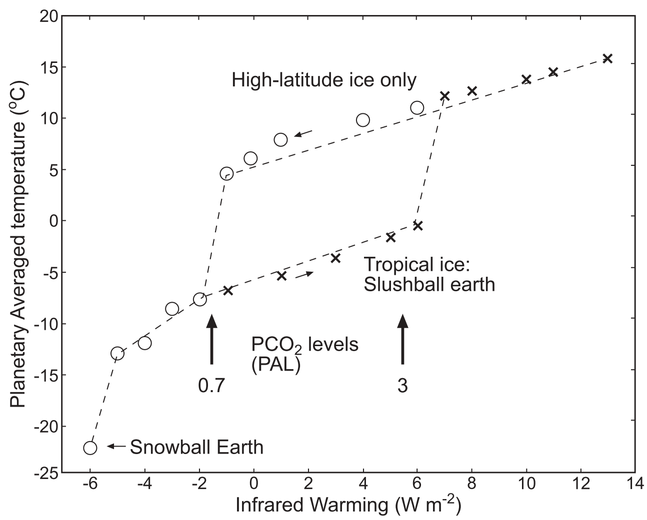

Fig. 13. Hysteresis plot (after Crowley *et al*. 2001) showing the existence of open-water (Slushball) solutions using an EBM connected to an ice-sheet model. ○, pathway starting from the non-glaciated state; ×, an initial Slushball state undergoing deglaciation. The exact position of the loop varies with modelled conditions and was shifted to lower $P\text{CO}_2$ values in the work of Peltier *et al*. (2004), who also showed another loop at the base of the diagram, representing Snowball deglaciation. The variations in radiative forcing lead to changes in atmospheric greenhouse gas forcing as shown, and so indicate the sensitivity of the system to biogeochemical feedbacks on $P\text{CO}_2$.

sea glaciers, the importance of even a weak hydrological cycle over long time scales and the possibility of enhanced seasonality. Given the lack of compelling geological evidence for the Snowball state, more modelling studies on the behaviours of Slushball Earth are needed. None yet have included all of dynamic atmosphere, ocean, sea ice and ice sheets (Jenkins 2004*a*; Poulsen & Jacob 2004), together with realistic topography, and the impact of dust (Pollard & Kasting 2005), clouds, and volcanic ash on albedo. In the short to medium term, models will still be strongly limited by the absence of good continental reconstructions. It will also be essential to work towards Earth System models that incorporate the biogeochemical feedbacks that are discussed in the next section.

Feedbacks affecting atmospheric compositions

The oxygen, sulphur and carbon global geochemical systems are linked through tectonically and biologically facilitated reactions that provide strong feedbacks to climate. It is our conjecture that the dramatic fluctuations and instabilities that characterize the Neoproterozoic biological, climatological and geochemical record are the symptoms of an emerging Earth System that becomes comparatively stabilized in the Phanerozoic. Before considering the history of the cycles, we demonstrate the principles in this section, via an illustration (Fig. 14) of the key positive and negative feedbacks of the Earth System that have been justified by quantitative models. Numbers in parentheses refer to fluxes and feedbacks in Figure 14.

Figure 14a focuses on the redox cycles, which have both direct and indirect relationships to climate. Oxygenation was crucial in allowing the evolutionary innovation of multicellular organisms (Canfield *et al*. 2006), while potentially shifting the Earth from a methane-modulated climate to the CO_2-feedback of the modern world. Hayes & Waldbauer (2006) have provided an elegant and rigorous account of the relationships between the deep Earth processes and those of the surface. For most of Earth history, a weakly reducing mixture of volcanic gases (mainly H_2O, CO_2, N_2 and H_2) has been emitted from volcanic sources, with H_2 continuously escaping to space (Catling & Claire 2005). Both S and Fe are primarily in reduced forms in primary volcanic products (1). A stepwise oxidation has occurred in Earth history, driven initially by the advent of photosynthesis, which dominates the production of free oxygen in the biosphere (1), stabilized by the long-term (10^7 years) accumulation of organic C in sediments, and made more permanent by subduction of this reduced C (1).

Oxygenic photosynthesis can be represented

$$CO_2 + H_2O \rightarrow CH_2O \quad \text{(organic C)} + O_2. \qquad (1)$$

In terms of mass balance, equation (1) is driven to the right only if there is an excess of photosynthesis over (aerobic) decay of organic matter, which on the geological time scale means an excess of organic carbon burial over oxidative weathering. The overall oxidation state of atmosphere and oceans is coupled to the abundance of available reduced species in those reservoirs (2). The most prominent negative feedbacks in this system are provided by the production and sequestration of organic carbon away from oxidants. For example, in modern (non-sulphidic) oceans this feedback is limited by P levels, which are controlled

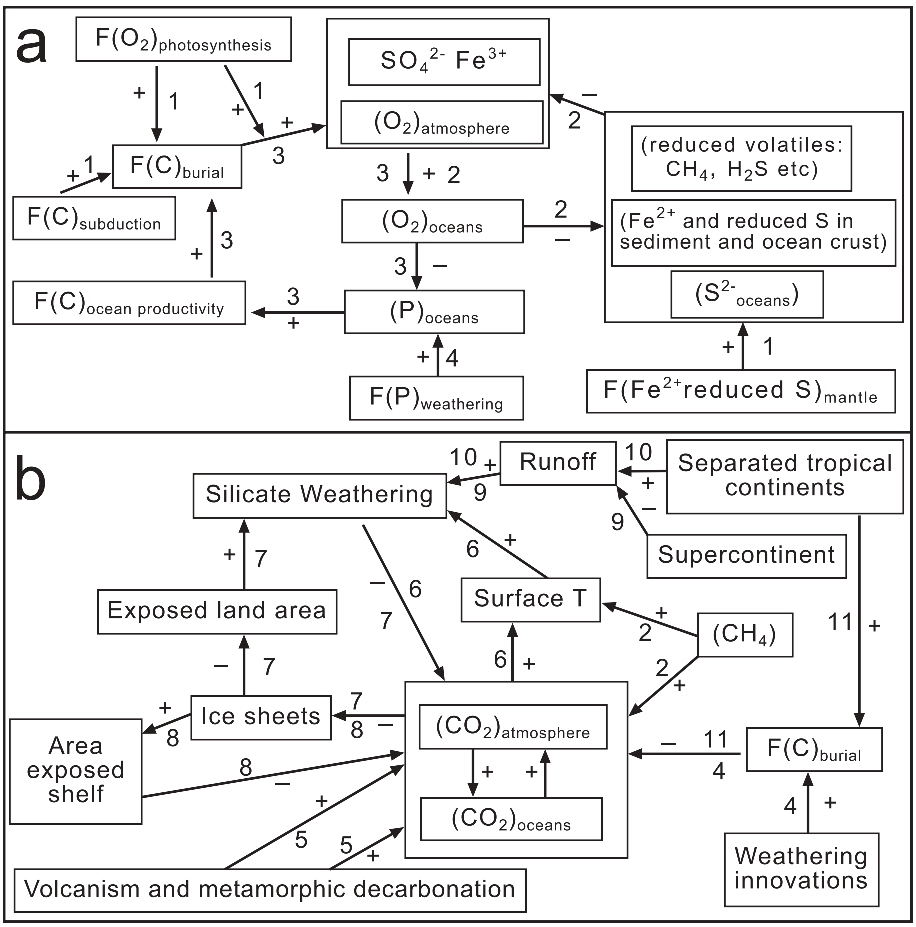

Fig. 14. Simplified overview of model-validated factors influencing (**a**) oxygenation and (**b**) carbon dioxide content of atmosphere and oceans. The factors are denoted as: (), concentrations; F(), fluxes. Positive influence is denoted by + and negative influence by –. A positive feedback loop is represented by an even number of negative signs, and a negative feedback loop by an odd number of negative signs. 1, primary drivers of mantle outgassing, subduction, and photosynthesis; 2, positive coupling of the atmosphere–ocean system in relation to the concentration of accessible reductants; 3, ocean productivity cycle with negative feedback on O_2; 4, external driver of intrinsic weathering efficiency, which relates to land biotas; 5, forcing by rate of degassing from Earth's interior; 6 and 7, negative feedbacks limiting PCO_2 changes (6, Walker feedback; 7, ice-sheet area feedback); 8, 'coral reef hypothesis' (i.e. less shelf area during glaciation reduces CO_2 output from carbonate formation); 9, supercontinent formation reduces runoff and silicate weathering; 10 and 11, break-up of tropical supercontinent reduces PCO_2 (10, by increasing runoff; 11, by increasing C burial around continental margins).

by strong adsorption on iron oxide particles, which limits productivity and hence carbon burial (3). Increased efficiency of P weathering (4) would increase the negative feedback effect, as has been modelled by Lenton & Watson (2004), based on evidence for a land biota evolving in early Neoproterozoic times. However, there is evidence for N, rather than P, to have been the key limiting nutrient in the Mesoproterozoic and at times in the Palaeozoic (Anbar & Knoll 2002; Saltzman 2005) and so there is uncertainty as to the coverage of the P mechanism. Also, most nutrients are recycled along continental margins in oceanic upwelling zones, rather than being directly controlled by primary weathering products dissolved in river runoff. Instead, more attention should be paid to burial efficiency of organic matter: another effect of land biota in the late Precambrian was to facilitate the generation of clay minerals to which organic molecules bind and are thus preserved (included in factor (4), Fig. 14b), elevating organic carbon burial efficiency to Phanerozoic levels (Kennedy *et al*. 2006).

The oxygen cycle is coupled to the CO_2 cycle and thus also plays a role in temperature regulation. For example, in Figure 14a, if an increase in the global oxidation potential reduced the residence time of atmospheric methane in the early Neoproterozoic (2), this would affect global temperature by reducing the overall greenhouse gas forcing. Because of the linkage between oxygen production and carbon burial in equation (1), times of cooling may be linked to enhanced marine productivity and/or burial of organic (reduced) carbon, requiring the withdrawal of atmospheric CO_2 and associated greenhouse-induced cooling. Rothman *et al*. (2003) called on the possible role of oxygenated cold glacial water in oxidizing part of a proposed large Neoproterozoic pool of dissolved organic carbon and hence giving rise to a rapid increase in PCO_2 and thus a negative feedback on glaciation. Peltier *et al*. (2004) argued that this may stabilize the modelled Slushball state, but the kinetics of this process have not been explored.

For the CO_2 cycle, long-term variations in CO_2 are anticipated; for example, by a general decline in deep Earth outgassing over time (Hayes & Waldbauer 2006), or by shorter-term variations in response to tectonic activity (5). The effect of initial colonization and expansion of a primitive land biota must have had a profound effect, as it plays such a critical role in the modern system. Terrestrial organisms would have increased the efficiency of weathering, enhancing the marine burial of C as discussed in the previous section (Mayer 1994; Lenton & Watson 2004; Kennedy *et al*. 2006) and also by increasing the rate at which CO_2 is removed from the atmosphere by silicate weathering (6). This accentuates the role of the feedback loop (6) by which PCO_2 is moderated (at least in areas of high relief, West *et al*. 2005) by the temperature-controlled rate of silicate weathering (Walker *et al*. 1981):

$$\text{silicates} + CO_2 \rightarrow \text{secondary silicates} + \text{aqueous silica} + \text{cations} + HCO_3^-. \tag{2}$$

On time scales of 10^7–10^8 years the CO_2 removed from the atmosphere is returned to the surface via release from the deep Earth (5) following subduction and metamorphism. Variations in carbonate weathering are not shown in Figure 14b because they are normally balanced by rates of $CaCO_3$ formation in the oceans, but during the deglaciation transient, high runoff may preferentially dissolve glacially ground carbonate rock flour (if available) rather than silicates because of their fast dissolution kinetics.

Two feedbacks are shown in Figure 14 relating to glaciation. A CO_2 fall inducing glaciation would lead to a negative feedback (7) whereby the coverage of land area by large ice sheets and the lower temperatures reduce chemical reaction rates of silicate weathering (Berner *et al*. 1983; Schrag *et al*. 2002), restoring CO_2 to the atmosphere. In contrast, a positive feedback arises through the effects of the developing ice sheets in causing a sea-level fall and hence increasing the area of exposed shelf (8). This shelf is now not available for $CaCO_3$ production, which was producing CO_2 by the reaction

$$Ca^{2+} + HCO_3^- \rightarrow CaCO_3 + CO_2 + H_2O. \tag{3}$$

In the Quaternary, this has the effect of greatly reducing the area of coral reef production, and hence was termed the coral reef hypothesis (Berger 1982). Times of reduced coral reef production drive an increase in carbonate saturation state and a consequent lowering of the lysocline of rapid deep-sea dissolution of pelagic carbonate. Ridgwell *et al*. (2003) used a C cycle model to quantify how much more important this mechanism was in Neoproterozoic times, in the absence of pelagic $CaCO_3$-secreting organisms and deep-sea carbonate compensation (Fig. 15). They

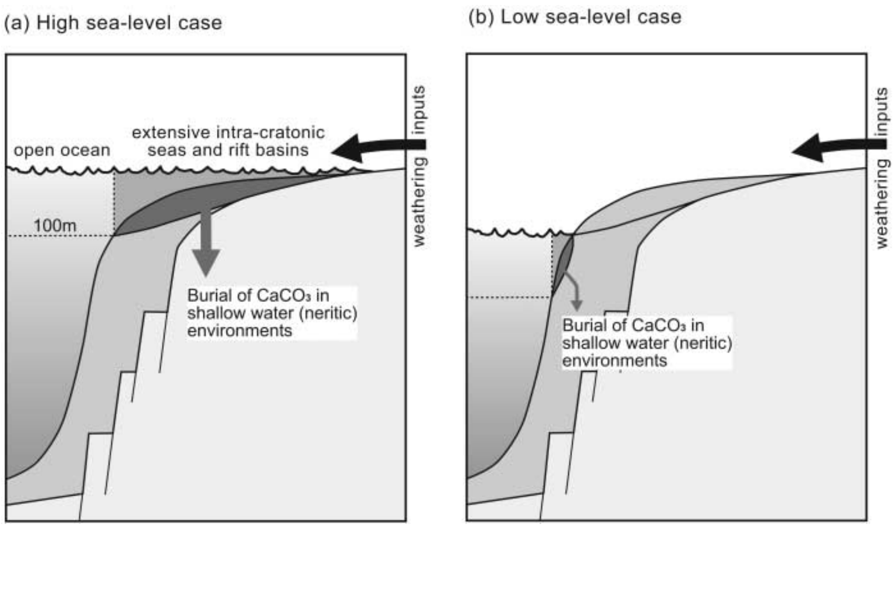

Fig. 15. Idealized Precambrian carbonate depositional system (Ridgwell & Kennedy 2004). (**a**) High sea level in steady state with weathering input of Ca^{2+} and HCO_3^- balanced by deposition of $CaCO_3$ in large neritic areas of rift and intracratonic basins. (**b**) Low sea level with reduced neritic area and hence lower rates of formation of $CaCO_3$ and associated CO_2 release to the atmosphere. This situation differs from Quaternary environments where the existence of planktonic carbonate-secreting organisms allows the changes in $CaCO_3$ production on shelves to be moderated by variations in the carbonate compensation depth and hence limits changes in atmospheric CO_2.

demonstrated the capacity of this mechanism to account for the anomalous variations in PCO_2 of *c*. 2500 ppm necessary to create low-latitude glaciation.

There are some good modelling constraints on the effects of palaeogeography. The creation of a supercontinent reduces global runoff and hence allows relatively high PCO_2 (9) regardless of its geographical position. However, an important study by Donnadieu *et al*. (2004) using an intermediate complexity climate model illustrated that the rifting of a tropical supercontinent into separate blocks maximizes runoff because of the high precipitation in the maritime tropics (10) and hence tends to increase weathering rates (Fig. 17). When coupled to a box model of the long-term C cycle, strong reduction in CO_2 is the consequence, which is accentuated when allowing for weathering of young volcanic rocks produced during rifting. Figure 16 illustrates that this has specifically been applied to a 750 Ma (Sturtian) palaeogeography. Schrag *et al*. (2002) argued that deltaic environments, favourable for organic C burial, would also occur more extensively in this palaeogeographical configuration (11). The efficacy of this source of organic carbon burial in the Proterozoic is unclear because of a much reduced flux of river-borne terrestrial biomass that contributes greatly to organic carbon delivery in Phanerozoic deltaic environments.

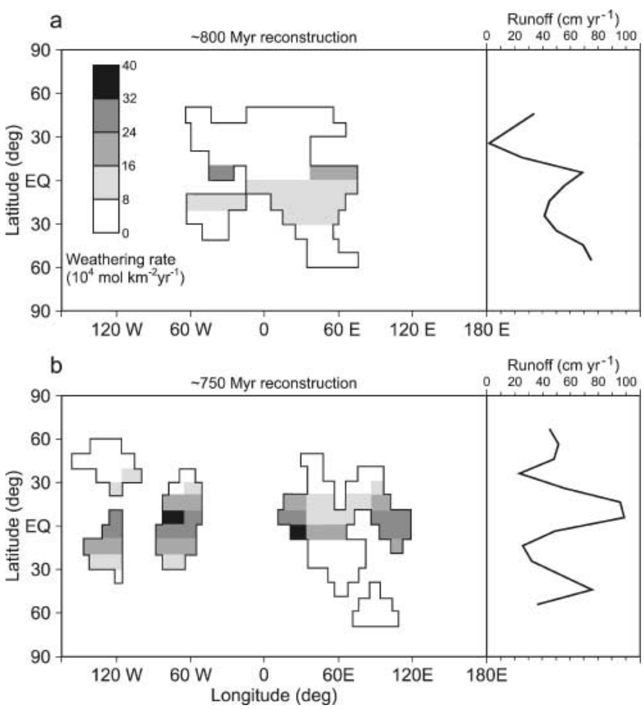

Fig. 16. Intermediate-complexity model runs indicating the impact of supercontinent fragmentation on rates of weathering and CO_2 drawdown (after Donnadieu *et al*. 2004). (**a**) 800 Ma reconstruction and (**b**) 750 Ma reconstruction, both at fixed PCO_2 of 1830 ppm. The increased continental freeboard and incidence of humid maritime climates results in substantially greater zonally averaged runoff from the continents at 750 Ma (lower right) compared with 800 Ma (upper right). The increased runoff is correlated with higher rates of chemical weathering. When coupled to a long-term carbon cycle box model, the PCO_2 at 800 Ma is stable at 1830 ppm (mean planetary temperature 10.8 °C), but that at 750 Ma drifts down to 510 ppm (mean temperature 2 °C). Studies using possible alternative continental positions and allowing for enhanced weathering of young basalts can lower PCO_2 to 250 ppm, under which conditions the model simulates runaway glaciation.

Neoproterozoic glaciation in Earth history

The foregoing discussion has highlighted a number of Earth System phenomena than could predispose the Earth to glaciation, or modify its effects. In Figure 17, we put the icehouse period of 750–580 Ma (the Neoproterozoic glacial era) in the context of the last 3 Ga of Earth history and ask why glaciation is temporally limited in this way. Notable changes across the era include the observed rise in $^{87}Sr/^{86}Sr$ (Fig. 17a), and the rise in atmospheric oxygen by its conclusion, inferred from biological and sulphur isotope data (Fig. 17d and e). The era itself is noted for disturbances to the carbon cycle, as manifested by $\delta^{13}C$ (Fig. 17c). Although orography, and ocean circulation in relation to high-latitude continents, influences the occurrence and intensity of glaciation, model results clearly show that widespread glaciation interrupting warmer climate must be associated with periods of low atmospheric PCO_2 (Fig. 17b), thus making the link to the global geochemical cycles of oxygen and carbon all the more likely.

The most plausible root causes for long-term change in the surface Earth System are deep Earth processes and biological innovation; for example, via their effect on master reactions (1) and (2). However, although reorganizations of mantle circulation might have resulted in stepwise reductions in outgassing and/or and changes in tectonic style, as proposed for example at 2.5–2.0 Ga (Kasting & Ono 2006) and around 1 Ga (Moores 2002), the evidence is disputed and so links are unclear. Similarly, there may be gaps of hundreds of millions of years between genomic changes permitting a new biological function and its quantitative impact. A good example (Fig. 17e) is the first appearance of sterane biomarkers for oxygenic photosynthesis from 2.7 Ga (Hayes & Waldbauer 2006; *contra* Kopp *et al*. 2005), well before evidence for significant accumulation of oxygen in the atmosphere in the Great Oxidation Event (Bekker *et al*. 2004).

Another fundamental change across the Neoproterozoic was the initial colonization of the land surface by fungi and photosynthetic microbes and algae (hence, probably, lichens). Terrestrial life has a strong influence on chemical weathering rates and related climate control feedbacks in the modern system, and so the initial colonization of the land surface might have resulted in a significant change. Evidence that this occurred in the early Neoproterozoic times is limited, but can be found in palaeokarstic surfaces (Horodyski & Knauth 1993), carbon isotope depletion in karstic profiles (Kenny & Knauth 2001), microbial mat textures in interfluve areas (Prave 2002), molecular clock evidence (Heckman *et al*. 2001), marine lichens (Yuan *et al*. 2005), and indirectly via changes in pedogenic clay mineral abundance in marine mud rocks (Kennedy *et al*. 2006). The resulting boost to silicate weathering rates toward modern values would have contributed to lowering atmospheric PCO_2 not only directly but also via increased nutrient supply to marine ecosytems (Lenton & Watson (2004) proposed selective P leaching from phosphates using organic acids) and through the biologically induced production of pedogenic clay minerals that act to preserve organic carbon within marine sediments (Mayer 1994; Kennedy *et al*. 2006). Enhanced organic carbon production and burial not only lowers PCO_2 and temperature, but increases atmospheric oxygen. Higher silicate weathering fluxes brought about by the expansion of a terrestrial biota also could account for stepwise rise in $^{87}Sr/^{86}Sr$ during the Neoproterozoic Glacial era (Fig. 17a), given the absence of a Himalayan-style orogen at the time (Kennedy *et al*. 2006). $^{87}Sr/^{86}Sr$ was not rising at the onset of Neoproterozoic glaciation, so any such biotic effects may have been masked at that time by the effects of supercontinental break-up, but in the period 750–500 Ma Kennedy *et al*. (2006) have shown a progressive rise in the phyllosilicate to tectosilicate ratio in Australian mudrocks, indicating progressively more effective chemical weathering processes and production of secondary clay minerals in primitive soils that corresponds to a step increase in marine $^{87}Sr/^{86}Sr$ suggestive of enhanced continental weathering.

A further coupling of climate to the carbon and oxygen cycles is via methane. Canfield (1998) argued that, at plausible levels of nutrient supply, the Mesoproterozoic ocean would have been pervasively anoxic below its surface. Methanogenesis of incompletely decomposed organic matter in such an ocean would significantly increase methane emissions and drive concentrations in the atmosphere as high as 100–300 ppm (compared with 1.7 ppb today) and warming by as much as 12 K (Pavlov *et al*. 2003; Kasting 2005). Methane thus probably played an important role in regulating planetary warmth. Catling & Claire (2005) calculated a significant oxidative effect during the Mesoproterozoic by the escape of H_2 from the atmosphere, sourced from methane, in addition to the net burial of organic C following the advent of photosynthesis. At some point in the Neoproterozoic, rising free oxygen concentrations in the biosphere must have significantly reduced the atmospheric concentration of methane (as methane rapidly oxidizes to CO_2 in the presence of O_2). Loss of the greenhouse warming effects of atmospheric methane might have been an important stimulus for initiation of glaciation (Schrag *et al*. 2002). Conversely, warming during deglaciation may have triggered the destabilization of methane clathrates, increasing atmospheric methane and acting as a positive feedback toward deglaciation (Ridgwell *et al*. 2003).

These arguments suggest that oxygen levels and Neoproterozoic climate may have been closely related and that the increase in atmospheric oxygen levels is at least coincidentally timed with Neoproterozoic ice ages. There are a few intriguing biological clues to oxygen levels during the Neoproterozoic. Canfield & Teske (1996) used biological 'clock' arguments for the origin of the sulphide-oxidizing organism *Beggiatoa*, which requires atmospheric oxygen >0.05 present atmospheric level by 750 Ma. The variability of sulphur isotopic values of pyrite and trace levels in carbonate becomes as great as in the Phanerozoic after the Marinoan, suggesting oxidation of the sulphide pool and significant microbially mediated sulphate oxidation of organic matter throughout the ocean (Ross *et al*. 1995; Kah *et al*. 2005). The volumetrically insignificant Banded Iron Formations found in association with a few Neoproterozoic glacial occurrences are likely to reflect local conditions in which deep-water anoxia may have been enhanced by ice cover (or by hydrothermal activity), rather than reflecting evidence for a global condition (see

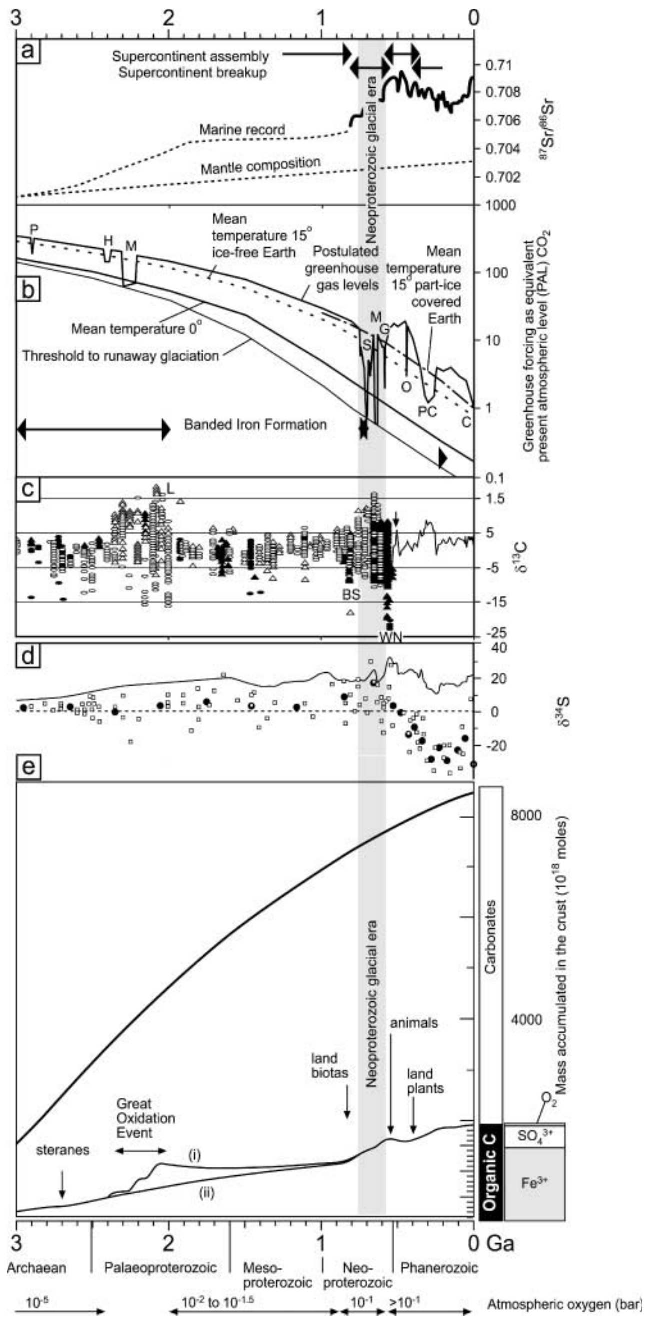

Fig. 17. The Neoproterozoic glacial era in its historical context. (**a**) Sr isotope marine record (Shields & Veizer 2002; Halverson *et al*. 2007). (**b**) Thresholds for climatic states at different temperatures from energy balance models of Tajika (2003, 2004), combined with Phanerozoic PCO_2 curve of Berner (1994) supplemented in the Ordovician and Precambrian by inferred variations in greenhouse forcing consistent with the glacial record. Glacial periods are: P, Pongola; H, Huronian; M, Makganyene; S, Sturtian; Ma, Marinoan; G, Gaskiers; O, Ordovician; PC, Permo-Carboniferous; C, Cenozoic. (**c**) Carbon isotope record; Proterozoic part is after Shields & Veizer (2002). Triangles are dolomite, ellipses are limestone. Open symbols have less certain age assignments. Proterozoic carbon isotope anomalies outside the glacial era: L, Lomagundi; BS, Bitter Springs; WN, Wonoka. (**d**) Record of $\delta^{34}S$ from sulphate (continuous line) compared with period averages (●) and formation averages (□) of pyrite (Canfield 2004). (**e**) Accumulation of crustal components and free oxygen (from material of Hayes & Waldbauer 2006), together with suggested atmospheric oxygen levels modified from Catling & Claire (2005) and marker events from various sources. Upper line illustrates accumulation of oxidized carbon (carbonates and CO_2) and organic carbon in the crust, derived from a model of net mantle CO_2 inputs over time. Lower lines (i) and (ii) illustrate models of accumulation of oxidized species to balance the accumulation of organic carbon, based on carbon isotope records of the balance of organic and carbonate C being accumulated at different times. Mean of present-day inventory estimates of oxidized species (Fe^{3+}, SO_4^{2-} and O_2) is shown at the right. It should be noted that Fe^{3+} refers only to that in excess of mantle Fe^{3+}/Fe^{2+} ratio of 0.12 and that the present-day atmospheric oxygen represents only around 2% of the total oxidants generated over time.

Hoffman & Schrag 2002). Hence, it is relevant to look more closely at the implications of C and S chemostratigraphy for atmospheric and ocean compositions, as they provide the most detailed and continuous records of environmental change.

A measure of the rate of permanent accumulation of reduced C in the crust can be gained by carbon isotope systematics. The CO_2 degassing from the mantle has a composition of close to −5‰ (Hayes & Waldbauer 2006). Over geological time periods this is balanced (Fig. 14a) by a mixture of isotopically heavy carbonates and strongly negative organic C generated by kinetic fractionations related to organic matter synthesis. If f_{carb} is the fraction of carbon removed as carbonates and f_{org} the fraction removed as organic C, then

$$f_{\text{carb}} = 1 - f_{\text{org}} \tag{4}$$

and isotopic mass balance requires that

$$\delta^{13}\text{C}_{\text{input}} = (1 - f_{\text{org}})\delta^{13}C_{\text{carb}} + f_{\text{org}}\delta^{13}C_{\text{org}}. \tag{5}$$

Over Earth history as a whole, the relative constancy of carbon isotope values of carbonates around 0‰ and organic carbon around −25‰ indicates that f_{org} has approximated 0.2, although the value is somewhat lower for the Precambrian, when organic matter is isotopically lighter (Des Marais *et al*. 1992; Hayes & Waldbauer 2006). During certain periods, such as in the immediate aftermath of Neoproterozoic glaciation, the long-term state may not apply; for example, there may be significant short-term methane release from a limited methane clathrate reservoir lowering $\delta^{13}C_{input}$ (Kennedy *et al*. 2001*a*; Jiang *et al*. 2003). Rothman *et al*. (2003) proposed a 10- to 100-fold higher dissolved organic carbon pool within Precambrian seawater compared with the value today, which constituted another pool of potentially unstable δ^{13}C-depleted reduced carbon capable of driving the oceanic dissolved inorganic carbon (DIC) δ^{13}C value negative if a significant component were rapidly oxidized. Also like methane, negative excursions related to oxidation of this pool (Fike *et al*. 2006) would be limited to the time during oxidation of this organic matter and hence this mechanism could not represent a steady-state condition of the ocean.

Figure 17c identifies two extended periods when significant deposits of carbonates with strongly positive δ^{13}C values of up 13‰ accumulated: the early Palaeoproterozoic and the Neoproterozoic. Such signatures are consistent with a 50–100% higher value of f_{org} and imply a higher than average rate of generation of oxidants (Fig. 17e, model line i). However, oceanographically, it is difficult to account for the conditions that could yield double global organic productivity and burial necessary to provide an f_{org} of 0.5. An alternative solution, however, maintains organic carbon burial flux constant but reduces the DIC pool (Bartley & Kah 2004).

By the Neoproterozoic, there is evidence at least locally for abundant reactive (reduced) Fe in non-sulphidic basinal sediments as a reductant (Fairchild *et al*. 2000; Canfield *et al*. 2006), but in other cases sulphide was important, so the unravelling of the S cycle becomes a key part of the problem. The sulphur system shows mass-dependent isotopic fractionations between oxidized and reduced forms, expressed as δ^{34}S, in an analogous way to the C cycle. A weakly oxidizing Mesoproterozoic atmosphere is associated with moderate degrees of fractionation between oxidized S (in carbonate-associated sulphate and in rare sulphate evaporites) and sulphides, arising from the kinetic fractionation associated with bacterial sulphate reduction. The Mesoproterozoic is also characterized by large, short-term stratigraphic variations of δ^{34}S (not visible on the scale of Fig. 17d) in shallow-water environments, which at 1.2–1.3 Ga yield modelled marine sulphate concentrations less than 15% of modern values (Kah *et al*. 2005). Such low sulphate can be related to small rates of pyrite weathering on land linked to low atmospheric oxygen (Pavlov *et al*. 2003). Nevertheless, Canfield (1998) argued that there was sufficient sulphate delivered by weathering to the oceans to generate a euxinic (both anoxic and sulphidic) deep ocean by reduction of sulphate to sulphide out of contact with the atmosphere. Hence it is the sulphide flux that removed Fe^{2+} and stopped the occurrence of Banded Iron Formation after 1.8 Ga (Fe^{2+} is quantitatively removed by S^{2-} in the form of pyrite). Kump & Seyfried (2005) showed that the Fe/S ratio of hydrothermal fluids increases at lower hydrostatic pressure and so could be influenced by low sea level during glaciation, implicating this, together with low oceanic sulphate, as a possible way of explaining the return of Banded Iron Formation in the Neoproterozoic.

Canfield & Teske (1996) found increasingly negative minimum values of δ^{34}S of sedimentary pyrite during the 1–0.6 Ga interval, pointing to redox S cycling and hence increased oxidation. Where the difference between pyrite and sulphate δ^{34}S values ($\Delta\delta^{34}$S) is >46‰ it implies disproportionation reactions (secondary reoxidation of sulphide to S^0, following by further reduction), rather than the maximum 40‰ fractionation from one-step reduction, and Anbar & Knoll (2002) argued for strong oxygenation through most of the Neoproterozoic on that basis. However, Figure 17d (Canfield 2004) shows a huge range of values of $\delta^{34}S_{pyrite}$ at a formation level indicating that robust conclusions about oxygenation are difficult to draw. Hurtgen *et al*. (2005) illustrated stratigraphic variability in both carbonate-hosted and pyrite-hosted S δ^{34}S values, and a lack of Δ^{34}S values >45 until *c*. 580 Ma; they proposed that earlier high Δ^{34}S values may be an artefact of high stratigraphic variability in $\delta^{34}S_{sulphate}$ associated with low sulphate concentrations. Future studies of δ^{34}S, with careful stratigraphic and petrographic control, have great potential to illuminate these issues, provided that the representativeness of strata in terms of being part of either a stratified ocean (Logan *et al*. 1995) or a well-mixed ocean can be defended.

New data (Canfield *et al*. 2006) show a sharp decrease in the proportion of reactive to total Fe in sediments after the time of the Gaskiers glaciation in Newfoundland associated with a broad decrease in δ^{34}S values, and imply a significant oxidation of deep oceans at the close of this glaciation. This was attributed to glacial input of nutrients and enhanced C burial, but even if this were to prove to be the proximate cause, it should be set against the longer-term pressures for oxygenation that we have discussed.

Conclusions

Geological observations provide evidence for two Neoproterozoic episodes of long-lived glaciation with ice in tropical palaeolatitudes, with geochronological constraints as yet insufficient to test the Snowball Earth prediction of intense glaciation with synchronous termination. However, there is already much evidence that the within-formation intensity of glaciation was variable over time, inconsistent with Snowball Earth. Also, there is no global δ^{13}C isotope anomaly prior to glaciation and the cap carbonates do not reflect exceptional rates of carbonate deposition, but rather reflect condensed sedimentation over periods encompassing several magnetic reversals. Hence the most specific of the geological evidence favouring the original formulation of Snowball Earth has been falsified, forcing increased reliance on the modelling argument of the strength of the ice–albedo feedback. Indeed, there are modelling difficulties in maintaining ice at sea level in the tropics for millions of years without freezing the planet, but coupling of climate models to biogeochemical models will help understand possible feedback mechanisms, such as the strong stabilizing effect on glaciation provided by sea-level fall, reducing CO_2 production by carbonate precipitation.

Neoproterozoic glaciation occurred within an era (750–580 Ma) that followed the break-up of an equatorial supercontinent and the initial development of a land biota, and represented a period of transition to a more oxic atmosphere. Several associated Earth System feedbacks would have tended to encourage lower greenhouse gas forcing, including weathering innovations and organic carbon burial, and progressive oxidation leading to a replacement of methane by carbon dioxide as the major greenhouse agent after water vapour. Whether an additional immediate and specific trigger is necessary (Schrag *et al.* 2002) to generate each of the two apparently more widespread glaciations is unclear. A better understanding from geochemical evidence of the history of oxygenation during the Neoproterozoic would be helpful, but future chemostratigraphic work needs to take more account of petrogenesis.

Although we have not considered biological evolution in this review, the evidence of increasing complexity through the Neoproterozoic, culminating in an explosion of metazoan diversity, is a key feature. The stepwise nature of the Neoproterozoic transition, as suggested by progressively rising $^{87}Sr/^{86}Sr$ signatures, seems most similar to the pattern of evolutionary addition, but whether these disturbances in the biosphere occurred as a response to the appearance of complex life or facilitated complex life is a critical question needing resolution. Detailed understanding of cause–effect relations are still largely lacking, hampered by the poor time-resolution of this period and the difficulty in correlation of incomplete records that need to be assembled to gain the necessary understanding. The next decade will provide exciting new developments in our understanding of the biogeochemical systems and the necessary developments needed to produce the life-support system necessary to support complex life. The great climate swings in the Neoproterozoic provide us with some of the most compelling evidence for this apparently necessary transition and pose the question of how much life has acted to bring its own environment into control: arguably Gaia has only a 'weak hand' (Leeder 2007). Even with only a partly frozen planet (Slushball Earth), rather than the deep-frozen Snowball, Neoproterozoic glacial events marked the most sustained, severe crisis in maintaining Earth's habitability since the intense meteoritic bombardments of its early Archaean days.

We thank P. Allen and J. Etienne for their convening of the Ascona symposium in July 2006, which provided an opportunity to discuss a wide range of current work. P. Allen, A. Prave and P. Smith are thanked for their reviews of the manuscript. M.J.K.'s current work is supported by NASA (NNG04GJ42G) and NSF (EAR 0345207). This is a contribution to IGCP Project 512.

References

Aitken, J.D. 1991a. Two Late Proterozoic glaciations, Mackenzie Mountains, northwestern Canada. *Geology*, **19**, 445–448.

Aitken, J.D. 1991b. *The Ice Brook Formation and post Rapitan Late Proterozoic glaciation, Mackenzie Mountains, Northwest Territories*. Geological Survey of Canada Bulletin, **404**.

Allen, P.A. & Hoffman, P.F. 2005. Extreme winds and waves in the aftermath of a Neoproterozoic glaciation. *Nature*, **433**, 123–127.

Amthor, J.E., Grotzinger, J.P., Schröder, S., Bowring, S.A., Ramezani, J., Martin, M.W. & Matter, A. 2003. Extinction of *Cloudina* and *Namacalathus* at the Precambrian–Cambrian boundary in Oman. *Geology*, **31**, 431–434.

Anbar, A.D. & Knoll, A.H. 2002. Proterozoic ocean chemistry and evolution: a bioinorganic bridge. *Science*, **297**, 1137–1142.

Arnaud, E. & Eyles, C.H. 2002. Catastrophic mass failure of a Neoproterozoic glacially influenced continental margin, the Great Breccia, Port Askaig Formation, Scotland. *Sedimentary Geology*, **151**, 313–333.

Arnaud, E. & Eyles, C.H. 2006. Neoproterozoic environmental change recorded in the Port Askaig formation, Scotland: climatic vs tectonic controls. *Sedimentary Geology*, **183**, 99–124.

Bartley, J.K. & Kah, L.C. 2004. Marine carbon reservoir, C_{org}–C_{carb} coupling, and the evolution of the Proterozoic carbon cycle. *Geology*, **32**, 129–132.

Baum, S.K. & Crowley, T.J. 2001. GCM response to late Precambrian (*c.* 590 Ma) ice-covered continents. *Geophysical Research Letters*, **28**, 583–586.

Bekker, A., Holland, H.D. & Wang, P.-L. et al. 2004. Dating the rise of atmospheric oxygen. *Nature*, **427**, 117–120.

Benn, D.I. & Prave, A.R. 2006. Subglacial and proglacial glacitectonic deformation in the Neoproterozoic Port Askaig Formation, Scotland. *Geomorphology*, **75**, 266–280.

Berger, W.H. 1982. Deglacial CO_2 buildup—constraints on the coral-reef model. *Palaeogeography, Palaeoclimatology, Palaeoecology*, **40**, 235–253.

Berner, R.A. 1994. Geocarb II: A revised model of atmospheric CO_2 over Phanerozoic time. *American Journal of Science*, **294**, 56–91.

Berner, R.A., Lasaga, A.C. & Garrels, R.M. 1983. The carbonate–silicate geochemical cycle and its effect on atmospheric carbon-dioxide over the past 100 million years. *American Journal of Science*, **283**, 641–683.

Besse, J. & Courtillot, V. 2002. Apparent and true polar wander and the geometry of the palaeomagnetic field over the last 200 Myr. *Journal of Geophysical Research*, **107**, 2300, doi:10.1029/2000JB000050.

Bodiselitch, B., Koeberl, C., Master, S. & Reimold, W.U. 2005. Estimating duration and intensity of Neoproterozoic Snowball Glaciations from Ir anomalies. *Science*, **308**, 239–242.

Bosak, T. & Newman, D.K. 2003. Microbial nucleation of calcium carbonate in the Precambrian. *Geology*, **31**, 577–580.

Bowring, S.A., Grotzinger, J.P., Isachsen, C.E., Knoll, A.H., Pelechaty, S.M. & Kolosov, P. 1993. Calibrating rates of Early Cambrian evolution. *Science*, **261**, 1293–1298.

Brady, P.V. & Gislason, S.R. 1997. Seafloor weathering controls on atmospheric CO_2 and global climate. *Geochimica et Cosmochimica Acta*, **61**, 965–973.

Brasier, M.D. & Shields, G. 2000. Neoproterozoic chemostratigraphy and correlation of the Port Askaig glaciation, Dalradian Supergroup of Scotland. *Journal of the Geological Society, London*, **157**, 909–914.

Brasier, M., McCarron, G., Tucker, R., Leather, J., Allen, P. & Shields, G. 2000. New U–Pb zircon dates for the Neoproterozoic Ghubrah glaciation and for the top of the Huqf Supergroup, Oman. *Geology*, **28**, 175–178.

Buchan, K.L., Ernest, R.E., Hamilton, M.A., Mertanen, S., Pesonen, L.J. & Elming, S.-Å. 2001. Rodinia: the evidence from integrated palaeomagnetism and U–Pb geochronology. *Precambrian Research*, **110**, 9–32.

Budyko, M.I. 1969. The effects of solar radiation variations on the climate of the Earth. *Tellus*, **XXI**, 611–619.

Caldeira, K. & Kasting, J.F. 1992. *Susceptibility of the early Earth to irreversible glaciation caused by carbon dioxide clouds.*, **359**, 226–228.

Canfield, D.E. 1998. A new model for Proterozoic ocean chemistry. *Nature*, **396**, 450–453.

Canfield, D.E. 2004. The evolution of the Earth surface sulphur reservoir. *American Journal of Science*, **304**, 839–861.

Canfield, D.E. & Teske, A. 1996. Late Proterozoic rise in atmospheric oxygen concentration inferred from phylogenetic and sulphur-isotope studies. *Nature*, **382**, 127–132.

Canfield, D.E., Poulton, S.W. & Narbonne, G.M. 2006. Late Neoproterozoic deep-ocean oxygenation and the rise of animal life. *Science*, doi: 10.1126/science.1135013.

Catling, D.C. & Claire, M.W. 2005. How Earth's atmosphere evolved to an oxic state: a status report. *Earth and Planetary Science Letters*, **237**, 1–20.

Cawood, P.A. 2005. Terra Australis Orogen: Rodinia breakup and development of the Pacific and Iapetus margins of Gondwana during the Neoproterozoic and Palaeozoic. *Earth-Science Reviews*, **69**, 249–279.

Clark, D.L., Whitman, R.R., Morgan, K.A. & Makey, S.D. 1980. *Stratigraphy and Glacial–Marine Sediments of the Amerasian Basin, Central Arctic Ocean*. Geological Society of America, Special Papers, **181**.

Cloud, P., Wright, L.A., Williams, E.G., Diehl, P. & Walter, M.R. 1974. Giant stromatolites and associated vertical tubes from Upper Proterozoic Noonday Dolomite, Death-Valley-Region, eastern California. *Geological Society of America Bulletin*, **85**, 1869–1882.

Coleman, A.P. 1926. *Ice Ages: Recent and Ancient*. Macmillan, London.

Condon, D. & Prave, A.R. 2000. U–Pb Two from Donegal: Neoproterozoic

glacial episodes on the northeast margin of Laurentia. *Geology*, **28**, 951–954.
Condon, D., Prave, A.R. & Benn, D.I. 2002. Neoproterozoic glacial rain-out intervals: observations and implications. *Geology*, **20**, 35–38.
Condon, D., Zhu, M., Bowring, S., Wang, W., Yang, A. & Jin, Y. 2005. U–Pb ages from the Neoproterozoic Doushantuo Formation, China. *Science*, **308**, 95–98.
Corsetti, F.A. & Grotzinger, J.P. 2005. Origin and significance of tube structures in Neoproterozoic post glacial cap carbonates: example from the Noonday Dolomite, Death Valley, United States. *Palaios*, **20**, 348–387.
Corsetti, F.A. & Kaufman, A.J. 2003. A complex microbiota from snowball Earth times: microfossils from the Neoproterozoic Kingston Peak Formation, Death Valley, USA. *Proceedings of the National Academy of Sciences of the US*, **100**, 4399–4404.
Craig, G.Y. (introducer) 1997. *The 1785 Abstract of James Hutton's Theory of the Earth*. Edinburgh University Library, Edinburgh.
Crossing, A.R. & Gostin, V.A. 1994. Isotopic signatures of carbonates associated with Sturtian (Neoproterozoic) glacial facies, central Flinders Ranges, South Australia. *In:* Deynoux, M., Miller, J., Domack, E., Eyles, N., Fairchild, I.J. & Young, G.M. (eds) *1994 Earth's Glacial Record*. Cambridge University Press, Cambridge, **1994**, 165–175.
Crowell, J.C. 1957. Origin of pebbly mudstones. *Geological Society of America Bulletin*, **68**, 993–1010.
Crowley, T.J., Hyde, W.T. & Peltier, W.R. 2001. CO_2 levels required for deglaciation of a 'Near-Snowball' Earth. *Geophysical Research Letters*, **28**, 283–286.
Dalziel, I.W.D. 1997. Neoproterozoic–Paleozoic geography and tectonics: review, hypothesis, environmental speculation. *Geological Society of America Bulletin*, **109**, 16–42.
Dempster, T.J., Rogers, G. & Tanner, P.W.G. *et al.* 2002. Sedimentary timing of deposition, orogenesis and glaciation within the Dalradian rocks of Scotland: constaints from U–Pb zircon ages. *Journal of the Geological Society, London*, **159**, 83–94.
Des Marais, D.J., Strauss, H., Simmons, R.E. & Hayes, J.M. 1992. Carbon isotope evidence for the stepwise oxidation of the Proterozoic environment. *Nature*, **359**, 605–609.
Deynoux, M. 1985. Terrestrial or waterlain glacial diamictites? Three case studies from the Late Precambrian and Late Ordovician glacial drifts in West Africa. *Palaeogeography, Palaeoclimatology, Palaeoecology*, **51**, 97–141.
Donnadieu, Y., Fluteau, F., Ramstein, G., Ritz, C. & Besse, J. 2003. Is there a conflict between the Neoproterozoic glacial deposits and the snowball Earth interpretation: an improved understanding with numerical modeling. *Earth and Planetary Science Letters*, **208**, 101–112.
Donnadieu, Y., Goddéris, Y., Ramstein, G., Nédélec, A. & Meert, J. 2004. A 'snowball Earth' triggered by continental break-up through changes in runoff. *Nature*, **428**, 303–306.
Dott, R.H. 1963. Dynamics of subaqueous gravity depositional processes. *AAPG Bulletin*, **47**, 104–128.
Dyson, I.A. & von der Borch, C.C. 1994. Sequence stratigraphy of an incised-valley fill: the Neoproterozoic Seacliff Sandstone, Adelaide Geosyncline, South Australia. *In:* Dalrymple, R.W., Boyd, R. & Zaitlin, B.A. (eds) *Incised-Valley Systems: Origin and sedimentary Sequences*. SEPM Special Publications, **51**, 209–222.
Eisbacher, G.H. 1985. Late Proterozoic rifting, glacial sedimentation and sedimentary cycles in the Windermere Supergroup, Mackenzie Moutains, northwestern Canada. *Palaeogeography, Palaeoclimatology, Palaeoecology*, **51**, 231–254.
Embleton, B.J.J. & Williams, G.E. 1986. Low palaeolatitudes of deposition for late Precambrian periglacial varvites in South Australia: implications for palaeoclimatology. *Earth and Planetary Science Letters*, **79**, 419–430.
Etienne, J.L., Allen, P.A., Rieu, R. & Le Guerroué, E. 2007. Neoproterozoic glaciated basins: a critical review of the Snowball Earth hypothesis by comparison with Phanerozoic glaciations. *In:* Hambrey, M.J., Christoffersen, P., Glasser, N.F. & Hubbard, B. (eds) *Glacial Processes and Products*. International Association of Sedimentologists, Special Publications, in press.
Evans, D.A.D. 2000. Stratigraphic, geochronological and paleomagnetic constraints upon the Neoproterozoic climatic paradox. *American Journal of Science*, **300**, 347–433.
Evans, D.A.D. 2003. True polar wander and supercontinents. *Tectonophysics*, **362**, 303–320.
Evans, D.A.D. 2006. Proterozoic low orbital obliquity and axial-dipolar geomagnetic field from evaporite palaeolatitudes. *Nature*, **444**, 51–55.
Eyles, C.H. & Eyles, N. 1983. A glaciomarine model for Upper Precambrian diamictites of the Port Askaig Formation, Scotland. *Geology*, **11**, 692–696.
Eyles, N. 1993. Earth's glacial record and its tectonic setting. *Earth-Science Reviews*, **35**, 1–248.
Eyles, N. & Januszczak, N. 2004. 'Zipper-rift': a tectonic model for Neoproterozoic glaciations during the breakup of Rodinia after 750 Ma. *Earth-Science Reviews*, **65**, 1–73.
Fairchild, I.J. 1991. Origins of carbonate in Neoproterozoic stromatolites and the identification of modern analogues. *Precambrian Research*, **53**, 281–299.
Fairchild, I.J. 1993. Balmy shores and icy wastes: the paradox of carbonates associated with glacial deposits in Neoproterozoic times. *In:* Wright, V.P. (ed.) *Sedimentology Review*, **1**, Blackwell Science, Oxford, 1–16.
Fairchild, I.J. & Hambrey, M.J. 1984. The Vendian succession of northeastern Spitsbergen—petrogenesis of a dolomite–tillite association. *Precambrian Research*, **26**, 111–167.
Fairchild, I.J. & Hambrey, M.J. 1995. Vendian basin evolution in East Greenland and NE Svalbard. *Precambrian Research*, **73**, 217–233.
Fairchild, I.J. & Spiro, B. 1987. Petrological and isotopic implications of some contrasting Late Precambrian carbonates, NE Spitsbergen. *Sedimentology*, **34**, 973–989.
Fairchild, I.J., Hambrey, M.J., Spiro, B. & Jefferson, T.H. 1989. Late Proterozoic glacial carbonates in northeast Spitsbergen: new insights into the carbonate–tillite association. *Geological Magazine*, **126**, 469–490.
Fairchild, I.J., Marshall, J.D. & Bertrand-Sarfati, J. 1990. Stratigraphic shifts in carbon isotopes from Proterozoic stromatolitic carbonates (Mauritania)—influences of primary mineralogy and diagenesis. *American Journal of Science*, **290A**, 46–79.
Fairchild, I.J., Bradby, L. & Spiro, B. 1994. Reactive carbonate in glacial systems: a preliminary synthesis of its creation, dissolution and reincarnation. *In:* Deynoux, M., Miller, J., Domack, E., Eyles, N., Fairchild, I.J. & Young, G.M. (eds) *1994 Earth's Glacial Record*. Cambridge University Press, Cambridge, **1994**, 176–192.
Fairchild, I.J., Spiro, B., Herrington, P.M. & Song, T. 2000. Controls on Sr and C isotope compositions of Neoproterozoic Sr-rich limestones of E Greenland and N China. *In:* Grotzinger, J.P. & James, N.P. (eds) *Carbonate Sedimentation and Diagenesis in the Evolving Precambrian World*. SEPM Special Publications, **67**, 297–313.
Fanning, C.M. & Link, P.K. 2004. U–Pb SHRIMP ages of Neoproterozoic (Sturtian) glaciogenic Pocatello Formation, southeastern Idaho. *Geology*, **32**, 881–884.
Fike, D.A., Grotzinger, J.P., Pratt, L.M. & Summons, R.E. 2006. Oxidation of the Ediacaran ocean. *Nature*, **444**, 744–747.
Frimmel, H.E., Klotzli, U.S. & Siegfried, P.R. 1996. New Pb–Pb single zircon constraints on the timing of Neoproterozoic glaciation and continental break-up in Namibia. *Journal of Geology*, **104**, 459–469.
Frisia, S. & Wenk, H.-R. 1994. TEM and AEM study of pervasive, multi-step dolomitization of the Upper Triassic Dolomia Principale (Northern Italy). *Journal of Sedimentary Petrology*, **63**, 1049–1058.
Gammon, P.R., McKirdy, D.M. & Smith, H.D. 2005. The timing and environment of tepee formation in a Marinoan cap carbonate. *Sedimentary Geology*, **177**, 195–208.
Goodman, J.C. 2006. Through thick and thin: marine and meteoric ice in a 'Snowball Earth' climate. *Geophysical Resesarch Letters*, **33**, L16701, doi:10.1029/2006GL026840.
Goodman, J.C. & Pierrehumbert, R.T. 2003. Glacial flow of floating marine ice in 'Snowball Earth'. *Journal of Geophysical Research*, **108**, 3308, doi:10.1029/2002JC001471.
Gross, M.G. & Tracey, J.I. 1966. Oxygen and carbon isotopic composition of limestones and dolomites, Bikini and Eniwatok atolls. *Science*, **151**, 1082–1084.
Grotzinger, J.P. & James, N.P. 2000. Precambrian carbonates: evolution of understanding. *In:* Grotzinger, J.P. & James, N.P. (eds) *Carbonate Sedimentation and Diagenesis in the Evolving Precambrian World*. SEPM Special Publications, **67**, 3–20.
Grotzinger, J.P. & Knoll, A.H. 1995. Anomalous carbonate precipitates: is the Precambrian the key to the Permian? *Palaios*, **10**, 578–596.
Grotzinger, J.P. & Knoll, A.H. 1999. Stromatolites in Precambrian carbonates: evolutionary mileposts or environmental dipsticks? *Annual Review of Earth and Planetary Sciences*, **27**, 313–358.
Halverson, G.P. 2006. A Neoproterozoic chronology. *In:* Xiao, S. & Kaufman, A.J. (eds) *Neoproterozoic Geobiology and Paleobiology*. Springer, New York, 231–271.
Halverson, G.P., Maloof, A.C. & Hoffman, P.F. 2004. The Marinoan glaciation (Neoproterozoic) in northeast Svalbard. *Basin Research*, **16**, 297–324.
Halverson, G.P., Hoffman, P., Schrag, D.P., Maloof, A.C. & Rice, A.H.N. 2005. Toward a Neoproterozoic composite carbon-isotope record. *Geological Society of America Bulletin*, **117**, 1181–1207.
Halverson, G.P., Dudás, F.Ö., Maloof, A.C. & Bowring, S.A. 2007. Evolution of the $^{87}Sr/^{86}Sr$ composition of Neoproterozoic seawater. *Palaeogeography, Palaeoclimatology, Palaeoecology*, doi: 10.1016/j.palaeo.2007.02.028.
Hambrey, M.J. & Harland, W.B. (eds) 1981. *Earth's Pre-Pleistocene Glacial Record*. Cambridge University Press, Cambridge.
Hambrey, M.J. & Harland, W.B. 1985. The late Proterozoic glacial era. *Palaeogeography, Palaeoclimatology, Palaeoecology*, **51**, 255–272.
Harland, W.B. 1964. Critical evidence for a great Infra-Cambrian glaciation. *Geologische Rundschau*, **54**, 45–61.

Harland, W.B. 2007. Origins and assessment of snowball Earth hypotheses. *Geological Magazine*, **144**, in press.

Harland, W.B. & Herod, K. 1975. Glaciations through time. *In:* Wright, A.E. & Moseley, F. (eds) *Ice Ages: Ancient and Modern*. Seel House Press, Liverpool, 189–216.

Harland, W.B. & Rudwick, M.J.S. 1964. The great infra-Cambrian ice age. *Scientific American*, **211**(2), 28–36.

Harland, W.B., Armstrong, R.L., Cox, A.V., Craig, L.E., Smith, A.G. & Smith, D.G. 1990. *A Geological Time Scale 1989*. Cambridge University Press, Cambridge.

Hayes, J.M. & Waldbauer, J.R. 2006. The carbon cycle and associated redox processes through time. *Philosophical Transactions of the Royal Society of London, Series B*, **361**, 931–950.

Heckman, D.S., Geiser, D.M., Eidell, B.R., Stauffer, R.L., Kardos, N.L. & Hedges, S.B. 2001. Molecular evidence for the early colonization of land by fungi and plants. *Science*, **293**, 1129–1133.

Hegenberger, W. 1993. *Stratigraphy and Sedimentology of the Late Precambrian Witvlei and Nama Groups, East of Windhoek*. Geological Survey of Namibia, Ministry of Mines and Energy, Memoir, **17**.

Higgins, J.A. & Schrag, D.P. 2003. Aftermath of a snowball Earth. *Geochemistry, Geophysics, Geosystems*, **4**, 1028, doi:10.1029/2002GC000403.

Hill, A.C., Arouri, K., Gorjan, P. & Walter, M.R. 2000. Geochemistry of marine and nonmarine environments of a Neoproterozoic cratonic carbonate–evaporite: the Bitter Springs Formation, Central Australia. *In:* Grotzinger, J.P. & James, N.P. (eds) *Carbonate Sedimentation and Diagenesis in the Evolving Precambrian World*. SEPM Special Publications, **67**, 327–344.

Hoffman, P.F. & Schrag, D.P. 2000. Snowball Earth. *Scientific American*, **282**(1), 50–57.

Hoffman, P.F. & Schrag, D.P. 2002. The snowball Earth hypothesis: testing the limits of global change. *Terra Nova*, **14**, 129–155.

Hoffman, P.F., Kaufman, A.J., Halverson, G.P. & Schrag, D.P. 1998. A Neoproterozoic Snowball Earth. *Science*, **281**, 1342–1346.

Hoffmann, K.-H., Condon, D.J., Bowring, S.A. & Crowley, J.L. 2004. U–Pb zircon date from the Neoproterozoic Ghuab Formation, Namibia: constraints on Marinoan glaciation. *Geology*, **32**, 817–820.

Horodyski, R.J. & Knauth, P. 1993. Life on land in the Precambrian. *Science*, **263**, 494–498.

Hurtgen, M.T., Arthur, M.A., Suits, N.S. & Kaufman, A.J. 2002. The sulphur isotopic composition of Neoproterozoic seawater sulfate: implications for a snowball Earth? *Earth and Planetary Science Letters*, **203**, 413–429.

Hurtgen, M.T., Arthur, M.A. & Halverson, G.P. 2005. Neoproterozoic sulphur isotopes, the evolution of microbial sulphur species, and the burial efficiency of sulphide as sedimentary pyrite. *Geology*, **33**, 41–44.

Hurtgen, M.T., Halverson, G.P., Arthur, M.A. & Hoffman, P.F. 2006. Sulfur cycling in the aftermath of a 635-Ma snowball glaciation: evidence for a syn-glacial sulfidic deep ocean. *Earth and Planetary Science Letters*, **245**, 551–570.

Hyde, W.T., Crowley, T.J., Baum, S.K. & Peltier, W.R. 2000. Neoproterozoic 'snowball Earth' simulations with a coupled climate/ice-sheet model. *Nature*, **405**, 425–429.

Ikeda, T. & Tajika, E. 1999. A study of the energy balance climate model with CO_2-dependent outgoing radiation: implication for the glaciation during the Cenozoic. *Geophysical Research Letters*, **26**, 349–352.

Jacobsen, S.B. & Kaufman, A.J. 1999. The Sr, C and O isootopic evolution of Neoproterozoic seawater. *Chemical Geology*, **161**, 37–57.

James, N.P., Narbonne, G.M. & Kyser, T.K. 2001. Late Neoproterozoic cap carbonates: Mackenzie Mountains, northwestern Canada: precipitation and global glacial meltdown. *Canadian Journal of Earth Sciences*, **38**, 1229–1262.

James, N.P., Narbonne, G.M., Dalrymple, R.W. & Kyser, T.K. 2005. Glendonites in Neoproterozoic low-latitude, interglacial sedimentary rocks, northwest Canada: insights into the Cryogenian ocean and Precambrian cold-water carbonates. *Geology*, **33**, 9–12.

Jenkins, G.S. 2004a. A review of Neoproterozoic climate modeling studies. *In:* Jenkins, G.S., McMenamin, M., Sohl, L.E. & McKay, C.P. (eds) *The Extreme Proterozoic: Geology, Geochemistry and Climate*. American Geophysical Union Monographs, **146**, 73–78.

Jenkins, G.S. 2004b. High obliquity as an alternative hypothesis to early and late Proterozoic extreme climate conditions. *In:* Jenkins, G.S., McMenamin, M., Sohl, L.E. & McKay, C.P. (eds) *The Extreme Proterozoic: Geology, Geochemistry and Climate*. American Geophysical Union Monographs, **146**, 183–192.

Jiang, G., Kennedy, M.J. & Christie-Blick, N. 2003. Stable isotopic evidence for methane seeps in Neoproterozoic postglacial cap carbonates. *Nature*, **426**, 822–826.

Jiang, G., Kennedy, M.J., Christie-Blick, N., Wu, H. & Zhang, S. 2006. Stratigraphy, sedimentary structures, and textures of the late Neoproterozoic Doushantuo cap carbonate in South China. *Journal of Sedimentary Research*, **76**, 978–995.

Kah, L.C., Lyons, T.W. & Frank, T.D. 2005. Low marine sulphate and protracted oxygenation of the Proterozoic biosphere. *Nature*, **431**, 834–838.

Kasemann, S.A., Hawkesworth, C.J., Prave, A.R., Fallick, A.E. & Pearson, P.N. 2005. Boron and calcium isotope composition in Neoproterozoic carbonate rocks from Namibia: evidence for extreme environmental change. *Earth and Planetary Science Letters*, **231**, 73–86.

Kasting, J.F. 2005. Methane and climate during the Precambrian era. *Precambrian Research*, **137**, 119–129.

Kasting, J.F. & Ono, S. 2006. Palaeoclimates: the first two billion years. *Philosophical Transactions of the Royal Society, Series B*, **361**, 917–929.

Kasting, J., Howard, M., Wallmann, K., Veizer, J., Shields, G. & Jaffrés, J. 2006. Paleoclimates, ocean depth, and the oxygen isotopic composition of seawater. *Earth and Planetary Science Letters*, **252**, 82–93.

Kaufman, A.J., Knoll, A.H. & Narbonne, G.M. 1997. Isotopes, ice ages, and terminal Proterozoic earth history. *Proceedings of the National Academy of Sciences of the USA*, **94**, 6600–6605.

Kaufman, A.J., Jiang, G., Christie-Blick, N., Banerjee, D.M. & Ria, V. 2006. Stable isotope record of the terminal Neoproterozoic Krol platform in the Lesser Himalayas of northern India. *Precambrian Research*, **147**, 156–185.

Kendall, B., Creaser, R.A. & Selby, D. 2006. Re–Os geochronology of post-glacial black shales in Australia: constraints on timing of 'Sturtian' glaciation. *Geology*, **34**, 729–732.

Kennedy, M.J. 1996. Stratigraphy, sedimentology, and isotopic geochemistry of Australian Neoproterozoic cap dolostones: deglaciation, $\delta^{13}C$ excursions, and carbonate precipitation. *Journal of Sedimentary Research*, **66**, 1050–1064.

Kennedy, M.J., Runnegar, B., Prave, A.R., Hoffman, K.-H. & Arthur, M.A. 1998. Two or four Neoproterozoic glaciations? *Geology*, **26**, 1059–1063.

Kennedy, M.J., Christie-Blick, N. & Sohl, L.E. 2001a. Are Proterozoic cap carbonates and isotopic excursions a record of gas hydrate destabilization following Earth's coldest intervals? *Geology*, **29**, 443–446.

Kennedy, M.J., Christie-Blick, N. & Prave, A.R. 2001b. Carbon isotopic composition of Neoproterozoic glacial carbonates as a test of paleoceanographic models for snowball Earth phenomena. *Geology*, **29**, 1135–1138.

Kennedy, M., Droser, M., Mayer, L.M., Pevear, D. & Mrofka, D. 2006. Late Precambrian oxygenation; inception of the clay mineral factory. *Science*, **311**, 1446–1449.

Kenny, R. & Knauth, L.P. 2001. Stable isotope variations in the Beck Spring Dolomite and Mesoproterozoic Mescal Limestone paleokarst; implications for life on land in the Precambrian. *Geological Society of America Bulletin*, **113**, 650–658.

Kirschvink, J.L. 1992. Late Proterozoic low-latitude glaciation. *In:* Schopf, J.W. (ed.) *The Proterozoic Biosphere*. Cambridge University Press, Cambridge, 51–52.

Knoll, A.H. & Swett, K. 1990. Carbonate deposition during the late Proterozoic era: an example from Spitsbergen. *American Journal of Science*, **290**, 104–132.

Knoll, A.H., Hayes, J.M., Kaufman, A.J., Swett, K. & Lambert, I.B. 1986. Secular variation in carbon isotope ratios from Upper Proterozoic successions of Svalbard and East Greenland. *Nature*, **321**, 832–838.

Knoll, A.H., Walter, M.R., Narbonne, G.M. & Christie-Blick, N. 2006. The Ediacaran Period: a new addition to the geologic time scale. *Lethaia*, **39**, 13–30.

Kopp, R.E., Kirschvink, J.L., Hilburn, I.A. & Nash, C.Z. 2005. The Paleoproterozoic snowball Earth: a climate disaster triggered by the evolution of oxygenic photosynthesis. *Proceedings of the National Academy of Sciences of the USA*, **102**, 11131–11136.

Kulling, O. 1934. Scientific results of the Swedish–Norwegian Arctic expedition in the summer of 1931. *Geografiska Annaler*, **2**, 161–254.

Kump, L.R. & Seyfried, W.E. 2005. Hydrothermal Fe fluxes during the Precambrian: effect of low oceanic sulfate concentrations and low hydrostatic pressure on the composition of black smokers. *Earth and Planetary Science Letters*, **235**, 654–662.

Land, L.S. 1973. Holocene meteoric dolomitization of Pleistocene limestones, North Jamaica. *Sedimentology*, **20**, 411–424.

Leather, J., Allen, P.A., Brasier, M.D. & Cozzi, A. 2002. Neoproterozoic snowball Earth under scrutiny: evidence form the Fiq glaciation of Oman. *Geology*, **30**, 891–894.

Leeder, M.R. 2007. Sedimentology, Cybertectonic Earth, sediment cycling and Gaia's weak pulse. *Journal of the Geological Society, London*, **164**, 277–296.

Lenton, T.M. & Watson, A.J. 2004. Biotic enhancement of weathering, atmospheric oxygen and carbon dioxide in the Neoproterozoic. *Geophysical Research Letters*, **31**, L05202, doi:10.1029/2003GL018802.

Levrard, B. & Laskar, J. 2003. Climate friction and the Earth's obliquity. *Geophysical Journal International*, **154**, 970–990.

Li, Z.X., Evans, D.A.D. & Zhang, S. 2004. A 90° spin on Rodinia: possible causal links between the Neoproterozoic supercontinent, superplume, true polar wander and low-latitude glaciation. *Earth and Planetary Science Letters*, **220**, 409–421.

Lindsay, J.F. 1989. Depositional controls on glacial facies associations in a basinal setting, Late Proterozoic, Amadeus Basin, central Australia. *Palaeogeography, Palaeoclimatology, Palaeoecology*, **73**, 205–232.

Logan, G.A., Hayes, J.M., Hieshma, G.B. & Summons, R.E. 1995. Terminal Proterozoic reorganization of biogeochemical cycles. *Nature*, **376**, 53–56.

Loutit, T.S., Hardenbol, J., Vail, P.R. & Baum, G.R. 1988. Condensed sections: the key to age determination and correlation of continental margin sequences. *In:* Wilgus, C.K., Hastings, B.S., Kendall, C.G.S.C., Posamentier, H.W., Ross, C.A. & Van Wagoner, J.C. (eds) *Sea-level Changes: an Integrated Approach*. SEPM Special Publications, **42**, 183–213.

Lovelock, J. 1988. *The Ages of Gaia*. Oxford University Press, Oxford.

Lovelock, J. 2006. *The Revenge of Gaia*. Allen Lane, London.

Maloof, A.C., Kellogg, J.B. & Anders, A.M. 2002. Neoproterozoic sand wedges: crack formation in frozen soils under diurnal forcing during a snowball Earth. *Earth and Planetary Science Letters*, **204**, 1–15.

Maloof, A.C., Halverson, G.P., Kirschvink, J.L., Schrag, D.P., Weiss, B.P. & Hoffman, P.F. 2006. Combined paleomagnetic, isotopic, and stratigraphic evidence for true polar wander from the Neoproterozoic Akademikerbreen Group, Svalbard, Norway. *Geological Society of America Bulletin*, **118**, 1099–1124.

Marshall, H.G., Walker, J.C.G. & Kuhn, W.R. 1988. Long-term climate change and the geochemical cycle of carbon. *Journal of Geophysical Research*, **90**, 791–801.

Mawson, D. 1949. The late Precambrian ice-age and glacial record of the Bibliando Dome. *Journal and Proceedings of the Royal Society of New South Wales*, **82**, 150–174.

Mayer, L.M. 1994. Surface area control of organic carbon accumulation in continental shelf sediments. *Geochimica et Cosmochimica Acta*, **58**, 1271–1284.

McCay, G.A., Prave, A.R., Alsop, G.I. & Fallick, A.E. 2006. Glacial trinity: Neoproterozoic Earth history within the British–Irish Caledonides. *Geology*, **34**, 909–912.

McIntyre, D.B. & McKirdy, A. 2001. *James Hutton. The Founder of Modern Geology*. National Museums of Scotland, Edinburgh.

McKirdy, D.M., Burgess, J.M. & Lemon, N.M. *et al.* 2001. A chemostratigraphic overview of the late Cryogenian interglacial sequence in the Adelaide Fold–Thrust Belt, South Australia. *Precambrian Research*, **106**, 149–186.

Meert, J.G. & van der Voo, R. 1994. The Neoproterozoic (1000–540 Ma) glacial intervals: no more snowball earth? *Earth and Planetary Science Letters*, **123**, 1–13.

Melezhik, V.A., Gorokhov, I.M., Kuznetsov, A.B. & Fallick, A.E. 2001. Chemostratigraphy of Neoproterozoic carbonates: implications for 'blind dating'. *Terra Nova*, **13**, 1–11.

Moncrieff, A.C.M. & Hambrey, M.J. 1990. Marginal-marine glacial sedimentation in the late Precambrian succession of east Greenland. *In:* Dowdeswell, J.A. & Scourse, J.D. (eds) *Glacimarine Environments: Processes and Sediments*. Geological Society, London, Special Publications, **53**, 387–410.

Moores, E.M. 2002. Pre-1 Ga (pre-Rodinian) ophiolites: their tectonic and environmental implications. *Geological Society of America Bulletin*, **114**, 80–95.

Pavlov, A.A., Hurtgen, M.T., Kasting, J.F. & Arthur, M.A. 2003. Methane-rich Proterozoic atmosphere? *Geology*, **31**, 87–90.

Peltier, W.R., Tarasov, L., Vettoretti, G. & Solheim, L.P. 2004. Climate dynamics in deep time: modeling the 'Snowball Bifurcation' and assessing the plausibility of its occurrence. *In:* Jenkins, G.S., McMenamin, M., Sohl, L.E. & McKay, C.P. (eds) *The Extreme Proterozoic: Geology, Geochemistry and Climate*. American Geophysical Union Monographs, **146**, 107–124.

Pierrehumbert, R.T. 2002. The hydrologic cycle in deep-time climate problems. *Nature*, **419**, 191–198.

Pierrehumbert, R.T. 2004. High levels of carbon dioxide necessary for the termination of global glaciation. *Nature*, **429**, 646–649.

Pierrehumbert, R.T. 2005. Climate dynamics of a hard snowball Earth. *Journal of Geophysical Research*, **110**, D01111, doi:1029/2004JD005162.

Plumb, K.A. 1991. New Precambrian time scale. *Episodes*, **14**, 139–140.

Pollard, D. & Kasting, J.F. 2004. Climate–ice sheet simulations of Neoproterozoic glaciation before and after collapse to Snowball Earth. *In:* Jenkins, G.S., McMenamin, M., Sohl, L.E. & McKay, C.P. (eds) *The Extreme Proterozoic: Geology, Geochemistry and Climate*. American Geophysical Union Monographs, **146**, 91–105.

Pollard, D. & Kasting, J.F. 2005. Snowball Earth: a thin ice solution with flowing sea-glaciers. *Journal of Geophysical Research—Oceans*, **110**, article number C07010.

Poulsen, C.J. & Jacob, R.L. 2004. Factors that inhibit snowball Earth simulation. *Palaeoceanography*, **19**, PA4021, doi:10.1029/2004PA001056.

Prave, A.R. 2002. Life on land in the Proterozoic; evidence from the Torridonian rocks of northwest Scotland. *Geology*, **30**, 811–814.

Preiss, W.V., Walter, M.R., Coates, R.P. & Wells, A.T. 1978. Lithological correlation of the Adelaidean glaciogenic rocks in parts of the Amadeus, Ngalia & Georgina Basins. *Bureau of Mineral Resources, Journal of Australian Geology and Geophysics*, **3**, 43–53.

Raub, T.D., Evans, D.A.D. & Smirnov, A.V. 2007. Siliciclastic prelude to Elatina–Nuccaleena deglaciation: lithostratigraphy and rock magnetism through the base of the Ediacaran system. *In:* Vickers-Rich, P. & Komarower, P. (eds) *The Rise and Fall of the Ediacaran Biota*. Geological Society, London, Special Publications, **286**, 53–76.

Ridgwell, A. & Kennedy, M. 2004. Secular changes in the importance of neritic carbonate deposition as a control on the magnitude and stability of Neoproterozoic ice ages. *In:* Jenkins, G.S., McMenamin, M., Sohl, L.E. & McKay, C.P. (eds) *The Extreme Proterozoic: Geology, Geochemistry and Climate*. American Geophysical Union Monographs, **146**, 55–72.

Ridgwell, A.J., Kennedy, M.J. & Caldeira, K. 2003. Carbonate deposition, climate stability, and Neoproterozoic ice ages. *Science*, **302**, 859–862.

Riding, R. 2000. Microbial carbonates: the geological record of calcified bacterial–algal mats and biofilms. *Sedimentology*, **41**(Supplement 1), 179–214.

Ross, G.M., Bloch, J.D. & Krouse, H.R. 1995. Neoproterozoic strata of southern Canadian Cordillera and the isotopic evolution of seawater sulfate. *Precambrian Research*, **73**, 71–99.

Rothman, D.H., Hayes, J.M. & Summons, R.E. 2003. Dynamics of the Neoproterozoic carbon cycle. *Proceedings of the National Academy of Sciences of the USA*, **100**, 8124–8129.

Saltzman, M.R. 2005. Phosphorus, nitrogen, and the redox evolution of the Paleozoic oceans. *Geology*, **33**, 573–576.

Schermerhorn, L.J.G. 1974. Late Precambrian mixtites: glacial and/or nonglacial? *American Journal of Science*, **274**, 673–824.

Schmidt, P.W. & Williams, G.E. 1995. The Neoproterozoic climatic paradox: equatorial palaeolatitudes for Marinoan glaciation near sea level in South Australia. *Earth and Planetary Science Letters*, **134**, 107–124.

Schrag, D.P. & Hoffman, P. 2001. Life, geology and snowball Earth. *Nature*, **409**, 306.

Schrag, D.P., Berner, R.A., Hoffman, P. & Halverson, G.P. 2002. On the initiation of a snowball Earth. *Geochemistry, Geophysics, Geosystems*, **3**, doi:10.1029/2001GC000219.

Shields, G.A. 1999. Working towards a new stratigraphic calibration scheme for the Neoproterozoic–Cambrian. *Eclogae Geologicae Helveticae*, **92**, 221–233.

Shields, G.A. 2002. 'Molar-tooth microspar': a chemical explanation for its disappearance *c*. 750 Ma. *Terra Nova*, **14**, 108–113.

Shields, G.A. 2005. Neoproterozoic cap carbonates: a critical appraisal of existing models and the plumeworld hypothesis. *Terra Nova*, **17**, 299–310.

Shields, G.A. & Veizer, J. 2002. Precambrian marine carbonate isotope database: Version 1.1. *Geochemistry, Geophysics, Geosystems*, **3**, doi:10.1029/2001GC000266.

Smith, A.G. & Pickering, K.T. 2003. Oceanic gateways as a critical factor to initiate icehouse Earth. *Journal of the Geological Society, London*, **160**, 337–340.

Sohl, L.E., Christie-Blick, N. & Kent, D.V. 1999. Paleomagnetic polarity reversals in Marinoan (*ca*. 600 Ma) glacial deposits of Australia: implications for the duration of low-latitude glaciation in Neoproterozoic time. *Geological Society of America Bulletin*, **111**, 1120–1139.

Spencer, A.M. 1971. *Late Pre-Cambrian Glaciation in Scotland*. Memoirs of the Geological Society, London, **6**.

Sumner, D.Y. 2001. Decimeter-thick encrustations of calcite and aragonite on the sea floor and implications for Neoarchean and Neoproterozoic ocean chemistry. *In:* Altermann, W. (ed.) *Precambrian Sedimentary Environments*. International Associations of Sedimentologists, Special Publications, **33**, 107–120.

Swart, P.K. & Eberli, G. 2005. The nature of the δ^{13}C of periplatform sediments: implications for stratigraphy and the global carbon cycle. *Sedimentary Geology*, **175**, 115–129.

Tajika, E. 2003. Faint young Sun and the carbon cycle: implication for the Proterozoic global glaciations. *Earth and Planetary Science Letters*, **214**, 443–453.

Tajika, E. 2004. Analysis of carbon cycle system during the Neoproterozoic: implication for Snowball Earth events. *In:* Jenkins, G.S., McMenamin, M., Sohl, L.E. & McKay, C.P. (eds) *The Extreme Proterozoic: Geology, Geochemistry and Climate*. American Geophysical Union Monographs, **146**, 45–54.

Thomas, G.P. & Connell, R.J. 1985. Iceberg drop, dump, and grounding structures from Pleistocene, glacio-lacustrine sediments, Scotland. *Journal of Sedimentary Petrology*, **55**, 243–249.

Thompson, M.D. & Bowring, S.A. 2000. Age of the Squantum 'Tillite' Boston Basin, Massachusetts: U–Pb zircon constraints on terminal Neoproterozoic glaciation. *American Journal of Science*, **300**, 630–655.

Torsvik, T.H. 2003. The Rodinia jigsaw puzzle. *Science*, **300**, 1379–1381.

Trindade, R.I.F., Font, E., D'Agrella-Filho, A.S., Nogueira, A.C.R. & Riccomini, C. 2003. Low-latitude and multiple geomagnetic reversals in the Neoproterozoic Puga cap carbonate, Amazon craton. *Terra Nova*, **15**, 441–446.

Walker, D.A. 1996. *Carbonates in marine polar sediments: palaeoceanographic and diagenetic studies*. PhD thesis, University of Birmingham.

Walker, G. 2003. *Snowball Earth*. Bloomsbury, London.

Walker, J.C.G., Hays, P.B. & Kasting, J.F. 1981. A negative feedback mechanism for the long-term stabilization of Earths surface-temperature. *Journal of Geophysical Research—Oceans and Atmospheres*, **86**, 9776–9782.

Walter, M.R. & Bauld, J. 1983. The association of sulphate evaporates, stromatolitic carbonates and glacial sediments. Examples from the Proterozoic of Australia and the Cainozoic of Antarctica. *Precambrian Research*, **21**, 129–148.

Warren, S.G., Brandt, R.E., Grenfell, T.C. & McKay, C.P. 2002. Snowball Earth: ice thickness on the tropical ocean. *Journal of Geophysical Research—Oceans*, **107**, 3167, doi:10.1029/2001JC001123.

West, A.J., Galy, A. & Bickle, M. 2005. Tectonic and climatic controls on silicate weathering. *Earth and Planetary Science Letters*, **235**, 211–228.

Williams, G.E. 1972. Geological evidence relating to the origin and secular roation of the solar system. *Modern Geology*, **3**, 165–181.

Williams, G.E. 1975. Late Precambrian glacial climate and the Earth's obliquity. *Geological Magazine*, **112**, 441–465.

Williams, G.E. 1979. Sedimentology, stable-isotope geochemistry and palaeoenvironment of dolostones capping late Precambrian glacial sequences in Australia. *Journal of the Geological Society of Australia*, **26**, 377–386.

Williams, G.E. 1993. History of the Earth's obliquity. *Earth-Science Reviews*, **34**, 1–45.

Williams, G.E. 2000. Geological constraints on the Precambrian history of Earth's rotation and the Moon's orbit. *Reviews of Geophysics*, **38**, 37–59.

Williams, G.E. & Schmidt, P.W. 2004. Neoproterozoic glaciation: reconciling low palaeolatitudes and the geologic record. *In:* Jenkins, G.S., McMenamin, M., Sohl, L.E. & McKay, C.P. (eds) *The Extreme Proterozoic: Geology, Geochemistry and Climate*. American Geophysical Union Monographs, **146**, 145–159.

Williams, G.E. & Tonkin, D.G. 1985. Periglacial structures and palaeoclimatic significance of a late Precambrian block field in the Cattle Grid copper mine, Mount Gunson, South Australia. *Australian Journal of Earth Sciences*, **32**, 287–300.

Wright, D.T. & Oren, A. 2005. Nonphotosynthetic bacteria and the formation of carbonates and evaporites through time. *Geomicrobiology Journal*, **22**, 27–53.

Young, G.M. 1984. Proterozoic plate-tectonics in Canada with emphasis on evidence for a late Proterozoic rifting event. *Precambrian Research*, **25**, 233–256.

Young, G.M. 2002. Stratigraphic and tectonic settings of Proterozoic glaciogenic rocks and banded iron-formations: relevance to the snowball Earth debate. *Journal of African Earth Sciences*, **35**, 451–466.

Yuan, X., Xiao, S. & Taylor, T.N. 2005. Lichen-like symbiosis 600 million years ago. *Science*, **308**, 1017–1020.

Received 12 December 2006; revised typescript accepted 1 March 2007.
Scientific editing by Rob Strachan